PLOS | ONE

Dopamine Modulates Acetylcholine Release via Octopamine and CREB Signaling in *Caenorhabditis elegans*

Satoshi Suo*, Shoichi Ishiura

Department of Life Sciences, Graduate School of Arts & Sciences, University of Tokyo, Tokyo, Japan

Abstract

Animals change their behavior and metabolism in response to external stimuli. cAMP response element binding protein (CREB) is a signal-activated transcription factor that enables the coupling of extracellular signals and gene expression to induce adaptive changes. Biogenic amine neurotransmitters regulate CREB and such regulation is important for long-term changes in various nervous system functions, including learning and drug addiction. In *Caenorhabditis elegans*, the amine neurotransmitter octopamine activates a CREB homolog, CRH-1, in cholinergic SIA neurons, whereas dopamine suppresses CREB activation by inhibiting octopamine signaling in response to food stimuli. However, the physiological role of this activation is unknown. In this study, the effect of dopamine, octopamine, and CREB on acetylcholine signaling was analyzed using the acetylcholinesterase inhibitor aldicarb. Mutants with decreased dopamine signaling exhibited reduced acetylcholine signaling, and octopamine and CREB functioned downstream of dopamine in this regulation. This study demonstrates that the regulation of CREB by amine neurotransmitters modulates acetylcholine release from the neurons of *C. elegans*.

Citation: Suo S, Ishiura S (2013) Dopamine Modulates Acetylcholine Release via Octopamine and CREB Signaling in *Caenorhabditis elegans*. PLoS ONE 8(8): e72578. doi:10.1371/journal.pone.0072578

Editor: Anne C. Hart, Brown University/Harvard, United States of America

Received March 17, 2013; **Accepted** July 10, 2013; **Published** August 16, 2013

Funding: This work was supported by JSPS Grant-in-Aid for Young Scientists (23700439) and for Scientific Research on Innovative Areas (Systems Molecular Ethology, 23115705). The funders had no role in study design, data collection and analysis, decision to publish, or preparation of the manuscript.

Competing Interests: The authors have declared that no competing interests exist.

* E-mail: suo@bio.c.u-tokyo.ac.jp

Introduction

The transcription factor cAMP response element binding protein (CREB) binds cAMP response element (CRE) and, upon activation by phosphorylation, induces the expression of downstream genes [1]. Biogenic amine neurotransmitters, including dopamine, serotonin, and norepinephrine, have been shown to regulate CREB activation through G protein-coupled receptors and G protein-mediated signaling [2,3]. The amine-mediated regulation of CREB plays important roles in many biological processes, including learning and drug addiction. CREB has been shown to regulate a large number of neuronally enriched genes, including genes that function in neurotransmitter or growth factor signaling, and genes encoding transcription or signal transduction factors [4]. These genes have important roles in the regulation of neuronal development, plasticity, and protection, and, although the precise mechanisms are not entirely known, CREB induces long-term changes in the condition of the neurons in which it is activated.

In the model animal *Caenorhabditis elegans*, the *crh-1* gene, which encodes CREB [5], is required for long-term learning in various experimental paradigms, as seen in other animals [6–9]. *crh-1* also controls the expression of *tph-1*, which is required for serotonin synthesis [10], and plays a role in the regulation of aging [11]. We previously showed that CREB was regulated by biogenic amines in *C. elegans* using the *cre::gfp* reporter [12,13], in which a CRE sequence is fused to GFP sequence. This reporter allows for the detection of CRE-mediated gene expression through GFP fluorescence in living animals [5]. Using this reporter system, we found that CREB was activated in all four cholinergic SIA neurons of *C. elegans* in the absence of food [12]. This activation is mediated by an amine neurotransmitter called octopamine, which is considered to be the biological equivalent of norepinephrine in invertebrates [14]. The octopamine receptor SER-3 and Gq alpha subunit EGL-30 function in SIA neurons to induce activation of the CREB homolog CRH-1. We subsequently found that dopamine signaling, which is believed to be activated in the presence of food in *C. elegans*, suppressed CREB activation in SIA neurons by inhibiting octopamine signaling [13]. Dopamine works through the dopamine receptors DOP-2 and DOP-3 and Gi/o alpha subunit GOA-1 to suppress octopamine release from octopaminergic neurons as well as octopamine-induced signaling in SIA neurons. However, the physiological role of CREB activation in SIA neurons is unknown.

Since SIA neurons are known to be cholinergic [15], it is possible that CREB activation in these neurons plays a role in the regulation of acetylcholine signaling. In this study, we examined acetylcholine signaling by monitoring aldicarb sensitivity and found that the regulation of CREB activation by biogenic amines in SIA neurons modifies acetylcholine signaling.

Materials and Methods

Strains

The culturing and genetic manipulation of *C. elegans* were performed as described [16]. The alleles used in this study were;

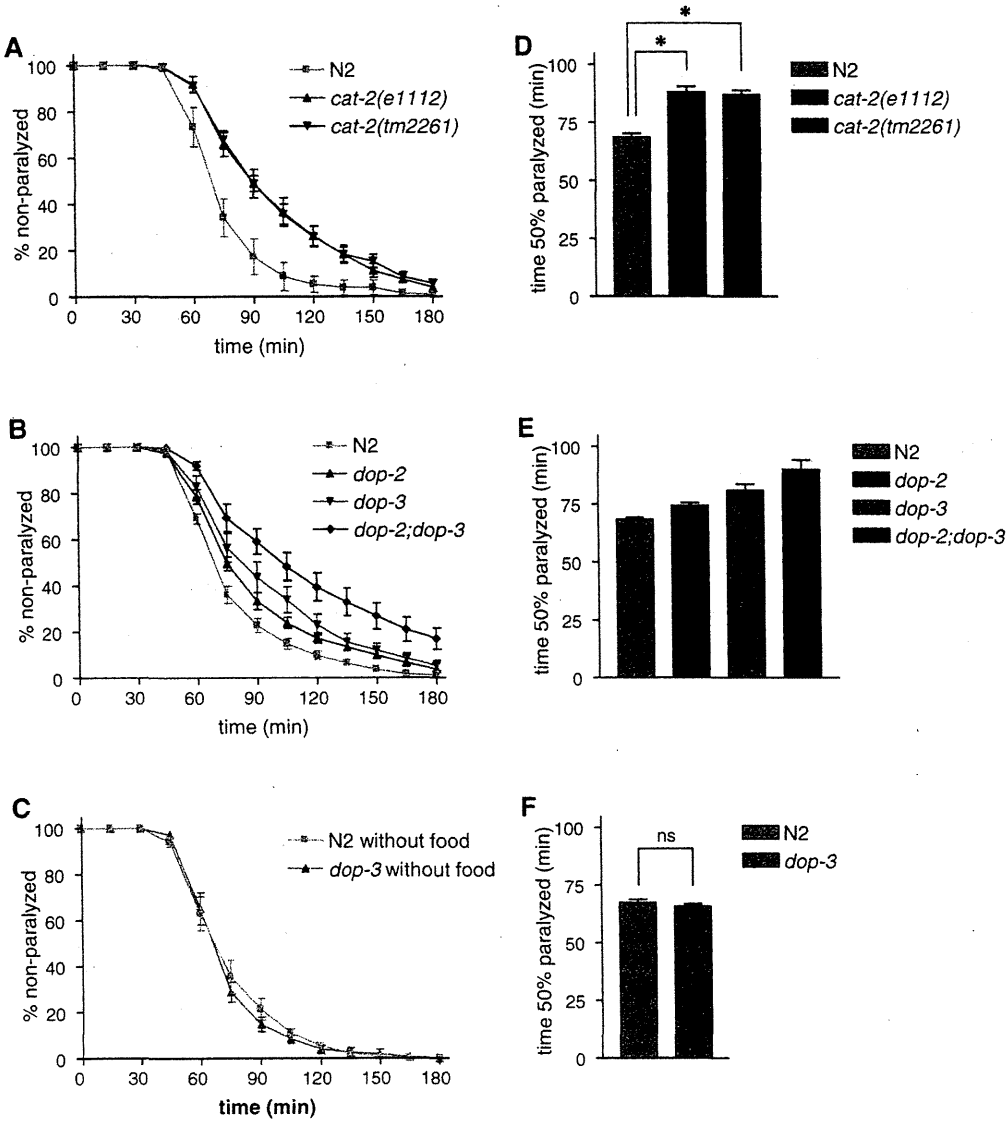

Figure 1. Dopaminergic mutants exhibit increased aldicarb resistance. (A-C) Animals were examined for paralysis on NGM plates containing 1 mM aldicarb. (D-F) The time required for 50% of the animals to become paralyzed was determined using Prism. (A and D) The dopamine-deficient *cat-2* mutants, *cat-2(e1112)* and *cat-2(tm2261)*, took longer to become paralyzed than wild-type N2 animals. *P<0.001 by the Tukey-Kramer multiple comparison test. (B and E) Aldicarb sensitivity of the *dop-2* and *dop-3* single mutants and *dop-2;dop-3* double mutant. Both *dop-2* and *dop-3* significantly increased aldicarb resistance ($F_{(1,28)}=9.52$, $p<0.01$ and $F_{(1,28)}=30.23$, $P<0.001$, respectively, by two-way ANOVA) without significant interaction ($F_{(1,28)}=0.37$, $P=0.55$ by two-way ANOVA). (C and F) The aldicarb resistance of N2 and *dop-3* mutant animals was measured in the absence of food. ns: $P>0.05$ by Student's *t*-test. Error bars indicate the SEM.
doi:10.1371/journal.pone.0072578.g001

ser-3(ad1774) I [12] (a gift from Drs. T. Niacaris and L. Avery, University of Texas Southwestern Medical Center, Dallas, TX), *cat-2(e1112) II* [17], *cat-2(tm2261) II* [18] (a gift from the National BioResource Project [NBRP], Ministry of Education, Culture, Sports, Science and Technology [MEXT], Tokyo, Japan), *crh-1(tz2) III* [5], *dop-2(vs105) V* [19], *tbh-1(ok1196) X* [12], and *dop-3(vs106) X* [19]. Double mutants were made using standard crossing techniques. The genotypes were confirmed by PCR for the deletion mutants and by PCR-RFLP for *cat-2(e1112)*.

Aldicarb and levamisole assays

The measurement of aldicarb and levamisole sensitivity was conducted as described [20] with some modifications. Aldicarb (AccuStandard Inc., New Haven, CT) and levamisole (Sigma-Aldrich, St. Louis, MO) were dissolved in DMSO and added to molten NGM agarose (standard NGM agar except that the agar was replaced by agarose) at a final concentration of 1 and 0.2 mM, respectively. Aliquots of 2 ml of each were transferred to 35-mm Petri dishes and allowed to solidify. An overnight culture of the bacterial strain OP50 in LB medium was diluted 20 times with water. A total volume of 20 µl of the diluted bacteria was then

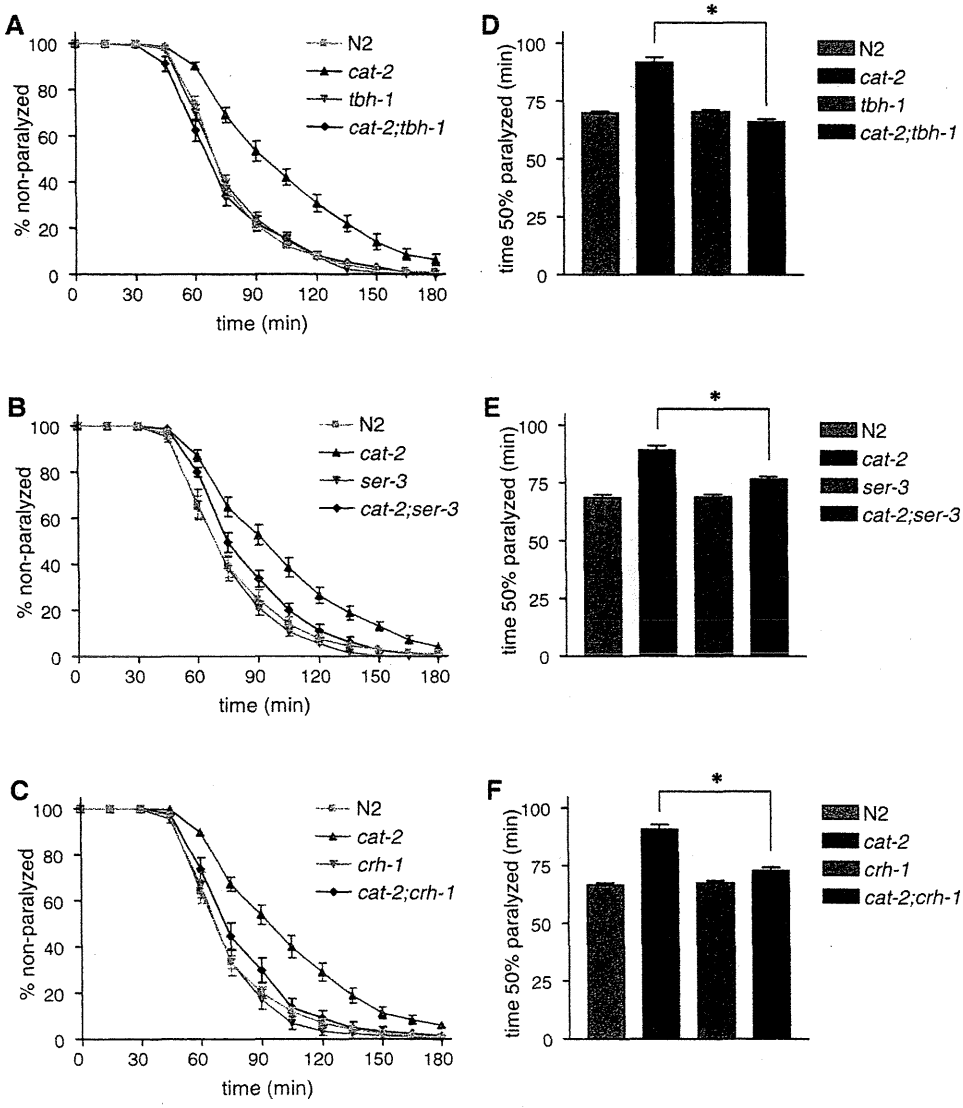

Figure 2. *tbh-1, ser-3,* and *crh-1* suppress *cat-2*. Double mutants for *cat-2* and *tbh-1* (A), *ser-3* (B), or *crh-1* (C) were examined for paralysis on NGM plates containing 1 mM aldicarb. (D-F) The time required for 50% of the animals to become paralyzed was determined using Prism. *tbh-1*, *ser-3*, and *crh-1* single mutants exhibited similar aldicarb sensitivity to wild-type N2 animals. The aldicarb resistance observed in the *cat-2* mutant was significantly reduced in the *cat-2;tbh-1*, *cat-2;ser-3*, and *cat-2,crh-1* double mutants. *P<0.001 by the Tukey-Kramer multiple comparison test. Error bars indicate the SEM.
doi:10.1371/journal.pone.0072578.g002

spread over the plates, except when the animals were tested in the absence of food. The plates were allowed to dry without lids for at least 1 h and stored at 20°C overnight to grow the bacteria. To prepare the animals used in the assays, an adult animal was placed on an NGM plate seeded with OP50. The plate was incubated at 20°C for 4 days to allow most of the F1s to become adults. Approximately 25 adult animals on the culture plates were transferred with a platinum wire to an aldicarb or levamisole assay plate. The animals were examined every 15 min and scored as paralyzed if they did not move after being prodded with a platinum wire. The experimenter was blinded to the genotypes of the tested animals. Each assay was done in duplicate and repeated at least four times.

Transgenic strains

The primers used for fusion gene construction were as follows (from 5′ to 3′):

A, ggatccaccggtaaaaatgatgttcctcagggcattac;

B, aagcttgcggccgctcacattccgtccttttccttttc; C, ctggaatcagtgttcttgttgc;

D, ctacaacggcagcgtattccgcctggaacagattgataaattc;

E, gtatgatgcgactattcagctgcgcctggaacagattgataaattc; F, gaatacgctgccgttg-tag;

G, cagctgaatagtcgcatcatac; H, caatgccatatcgggaaacc; I, gattg-agcccgaactttgaac; and

J, cacaagttcgtgcgtcaag.

The cDNA for *crh-1* was amplified using primers A and B from *cmk-1::crh-1* [5]. The amplified DNA was digested with *Age*I and *Not*I and cloned into *Age*I- and *Not*I-digested *ceh-17::dop-3fl* [13] to obtain

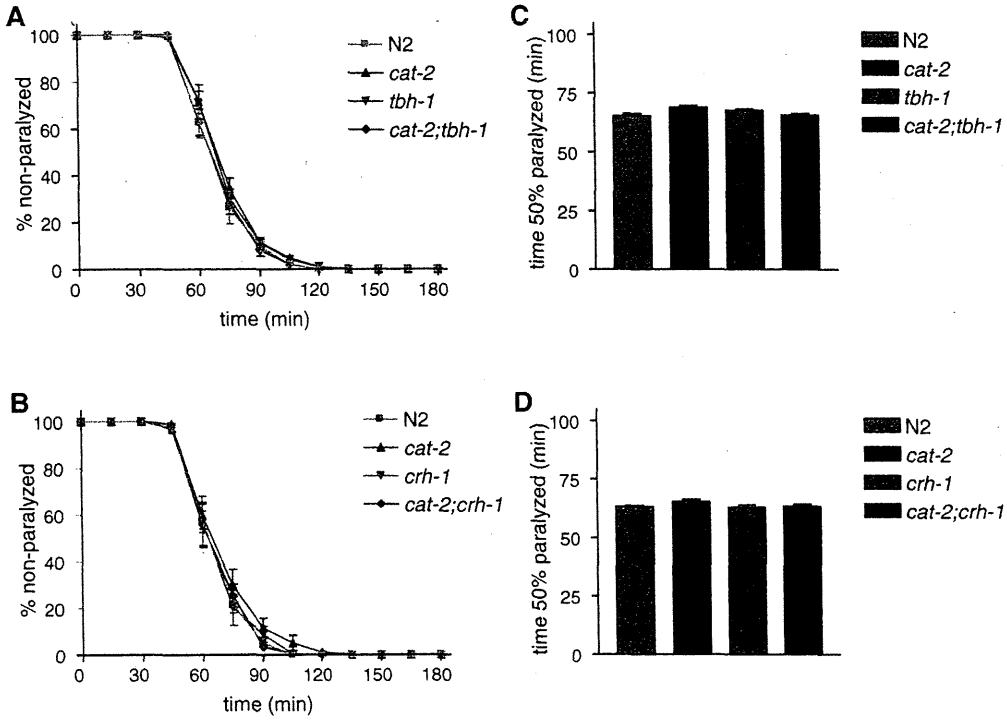

Figure 3. Levamisole sensitivity was unchanged in the *cat-2, tbh-1,* and *crh-1* mutants. (A and B) Animals were examined for paralysis on NGM plates containing 0.2 mM levamisole. (C and D) The time required for 50% of the animals to become paralyzed was determined using Prism. A one-way ANOVA revealed that *cat-2, tbh-1,* or *crh-1* mutation does not significantly alter levamisole sensitivity ($P>0.05$). Error bars indicate the SEM.
doi:10.1371/journal.pone.0072578.g003

ceh-17::crh-1. Next, *ceh-17::crh-1* was injected into *cat-2(e1112);crh-1(tz2)* together with a transformation marker, *lin-44::gfp* [21], which induces GFP expression in the tail, and pBlueScript (Invitrogen, Carlsbad, CA). In the aldicarb assays, the progeny of a transgenic animal were tested and those animals that carried the transgene and exhibited GFP expression were scored separately from those animals that had lost the transgene and did not show GFP expression. *cat-2(e1112);crh-1(tz2)* was injected only with *lin-44::gfp* and pBlueScript and this transgenic strain was tested as a control.

The fusion genes used for the SIA neuron-specific RNAi of the *cha-1* gene were made as described by Esposito et al [22]. Primers C and D or C and E were used to amplify the *ceh-17* promoter region from *ceh-17::dop-3*, and primers F and G were used to amplify part of the *cha-1* coding region from genomic DNA. The amplified DNAs were mixed and fusion genes were obtained using primers H and I or H and J. The fusion genes were mixed and injected into N2 and *cat-2(e1112)* mutant animals together with *lin-44::gfp* and pBlueScript. The GFP-expressing transgenic animals were used for the aldicarb assays.

Statistical analyses

The time required for 50% of the animals to become paralyzed (T_{50}) was calculated with Prism software (GraphPad Software, San Diego, CA) by a non-linear regression analysis of the Boltzmann sigmoidal curve, as described previously for a *C. elegans* killing assay [23]. To compare the T_{50} among strains, the statistical significance was evaluated by a one-way ANOVA followed by the Tukey-Kramer multiple comparison test using Prism software, except for Figure 1E and 1F, which were evaluated by a Student's *t*-test and a two-way ANOVA, respectively.

Results and Discussion

Suppression of dopamine signaling reduces acetylcholine signaling

In *C. elegans*, the relative strength of acetylcholine signaling can be measured by monitoring the paralyzing effect of the acetylcholinesterase inhibitor aldicarb [20]. Animals with a reduced level of acetylcholine signaling exhibit enhanced resistance to aldicarb, whereas animals with increased acetylcholine signaling are hypersensitive to it. To determine the effect of dopamine on acetylcholine signaling, we first analyzed the aldicarb sensitivity of *cat-2* mutants. The *cat-2* gene encodes tyrosine hydroxylase and is required for dopamine synthesis [24]. We analyzed two different alleles of *cat-2* and found that both mutants exhibited moderate resistance to aldicarb as they took significantly more time to become paralyzed than did wild-type N2 animals (Figure 1A and D). This result suggests that acetylcholine signaling was reduced in the *cat-2* mutants. The D2-like dopamine receptors DOP-2 [25] and DOP-3 [26] work downstream of dopamine in the regulation of CREB in SIA neurons [13]. We measured the aldicarb sensitivity of *dop-2* and *dop-3* single mutants as well as that of *dop-2;dop-3* double mutants (Figure 1B and E). A two-way ANOVA revealed that both the *dop-2* and *dop-3* mutations significantly increased the resistance of the animals to aldicarb ($F_{(1,28)} = 9.52$, $p<0.01$ and $F_{(1,28)} = 30.23$, $P<0.001$, respectively), whereas there was no significant interaction between the effects of *dop-2* and *dop-3* ($F_{(1,28)} = 0.37$, $P = 0.55$). These results suggest that the suppression of dopamine signaling results in reduced acetylcholine signaling.

Allen et al. reported that the *dop-3* mutant exhibits wild-type aldicarb sensitivity in the absence of food and that only in the enhanced background of *ace-1* does the *dop-3* mutation cause hypersensitivity to aldicarb [27], as opposed to resistance we observed in this study. The *ace-1* gene encodes acetylcholinesterase, which is released from muscle cells to degrade acetylcholine [28]. Therefore, *ace-1* mutants should have an increased level of acetylcholine in the neuromuscular junction. Allen et al. also showed that, for this hypersensitivity, *dop-3* works in the cholinergic motor neurons of the ventral cords [27]. The experiments in Figure 1B and E were conducted in the presence of food. Since aldicarb sensitivity is influenced by the experimental conditions [20], we also analyzed the aldicarb sensitivity of wild-type and *dop-3* animals in the absence of food and found that the *dop-3* mutant exhibited similar aldicarb sensitivity to wild-type animals in this condition (Figure 1C), which is consistent with the previous study. Our finding that *dop-3* mutants exhibit stronger aldicarb resistance than wild type animals only in the presence of food suggests that food availability influences the effect of dopamine on acetylcholine signaling. This is in line with the reports that dopamine signaling works in the presence of food to induce behavioral changes in *C. elegans* [19,29].

The aldicarb resistance of *cat-2* is suppressed by *tbh-1*, *ser-3*, and *crh-1*

With respect to the regulation of CREB activation in SIA neurons, octopamine signaling works downstream of dopamine [13]. We previously showed that octopamine signaling was activated in the *cat-2* mutant, and that spontaneous CREB activation in the *cat-2* mutant was suppressed by a mutation in the *tbh-1* gene, which encodes tyramine β-hydroxylase and is required for octopamine production [30]. To determine whether octopamine signaling also works downstream of dopamine in the regulation of acetylcholine signaling, we examined the effect of the *tbh-1* mutation in the regulation of aldicarb sensitivity (Figure 2A and D). The aldicarb sensitivity of the *tbh-1* mutant was not different from that of wild-type animals. The *cat-2;tbh-1* double mutant also exhibited normal aldicarb sensitivity, indicating that the aldicarb resistance observed in the *cat-2* mutant was completely suppressed by the mutation of *tbh-1*. Since the octopamine receptor SER-3 is required for octopamine-mediated CREB activation in SIA neurons [12], we next analyzed the *ser-3* mutant and found that *ser-3* also, albeit partially, suppressed the aldicarb resistance of *cat-2* (Figure 2B and E). To determine whether CREB plays a role in the regulation of acetylcholine signaling, we analyzed *crh-1* mutants. *crh-1* encodes a CREB homolog that is required for CRE-mediated gene expression [12]. *crh-1*, similar to *ser-3*, suppressed the enhanced aldicarb resistance observed in the *cat-2* mutants (Figure 2C and F), suggesting that *crh-1* also works downstream of *cat-2*. Taken together, these results suggest that the same pathway that works in the regulation of CRE-mediated gene expression in SIA neurons functions in the regulation of acetylcholine signaling.

Aldicarb causes the accumulation of acetylcholine in the synaptic cleft, leading to the over-activation of cholinergic receptors on muscle and paralysis [20]. Aldicarb resistance could result from decreased acetylcholine release from neurons or from decreased acetylcholine sensitivity of the muscles. To distinguish between these possibilities, we measured the sensitivity of the mutants to levamisole, an agonist of muscle acetylcholine receptors [31]. Sensitivity to levamisole was largely unchanged in the *cat-2*, *tbh-1*, and *crh-1* mutants as well as the *cat-2;tbh-1* and *cat-2;crh-1* double mutants (Figure 3). These results suggest that the aldicarb resistance observed in the *cat-2* mutant was caused by decreased acetylcholine release from neurons rather than a change in sensitivity to acetylcholine.

CRH-1 works in SIA neurons to regulate aldicarb sensitivity

Using the *cre::gfp* reporter, we previously showed that SIA neurons are the only cells in which CREB activity is detectably regulated by *cat-2* [13]. To examine whether SIA neurons are indeed where CREB functions in the regulation of acetylcholine signaling by dopamine, we conducted the cell-specific rescue of *crh-1* in *cat-2;crh-1* double mutants. If *crh-1* functions in SIA neurons, the expression of *crh-1* only in these cells should increase the aldicarb resistance of *cat-2;crh-1* double mutants. For this purpose, *crh-1* was expressed under the *ceh-17* promoter (*ceh-17::crh-1*) [32], which induces gene expression only in SIA neurons and one additional neuron (the ALA neuron). The *cat-2;crh-1*

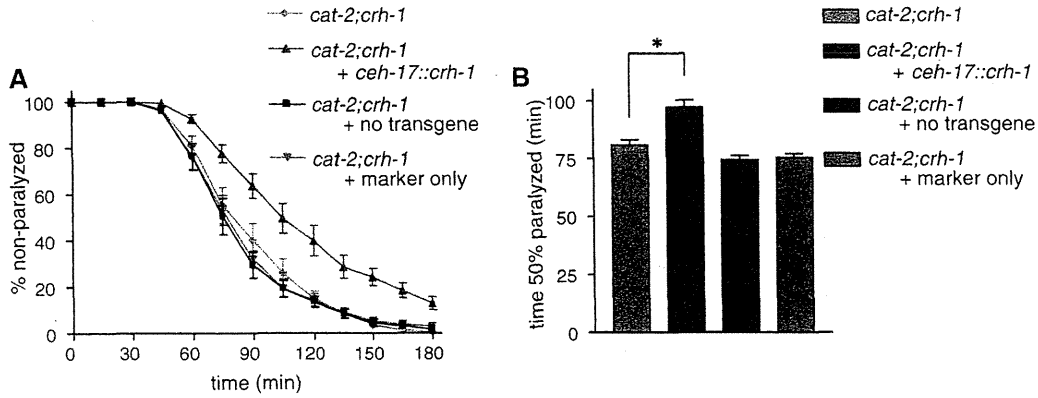

Figure 4. *crh-1* expression in SIA neurons rescued aldicarb resistance in the *cat-2;crh-1* double mutant. *cat-2;crh-1* mutants were transformed with *ceh-17::crh-1* and the co-injection marker *lin-44::gfp*. (A) Animals were examined for paralysis on NGM plates containing 1 mM aldicarb. (B) The time required for 50% of the animals to become paralyzed was determined using Prism. Animals carrying the transgene exhibited stronger aldicarb resistance than did the original double mutants. Those animals that lost the transgene or that were transformed only with the co-injection marker showed similar levels of aldicarb sensitivity to the *cat-2;crh-1* double mutants. *P<0.001 by the Tukey-Kramer multiple comparison test. Error bars indicate the SEM.
doi:10.1371/journal.pone.0072578.g004

double mutants carrying *ceh-17::crh-1* exhibited stronger aldicarb resistance compared to the original (*cat-2;crh-1*) double mutants, whereas control animals that had lost *ceh-17::crh-1* or that had been injected only with the co-injection marker did not (Figure 4). These results suggest that the expression of *crh-1* in SIA neurons is sufficient for the dopamine-mediated regulation of acetylcholine signaling.

It remained unclear whether a change in acetylcholine release from SIA neurons contributes to the regulation of aldicarb sensitivity by dopamine. To address this, we conducted the cell-specific RNAi-mediated knockdown of the *cha-1* gene, which encodes the choline acetyltransferase and is required for acetylcholine synthesis [33], using the *ceh-17* promoter. Animals with a wild-type background that were subjected to RNAi exhibited stronger aldicarb resistance than did wild-type animals, although it was not as strong as did the *cat-2* mutant (Figure 5).Considering that the ALA neuron is not cholinergic [15], this result suggests that the removal of acetylcholine from SIA neurons alone causes aldicarb resistance. If the aldicarb resistance observed in the *cat-2* mutant was due to reduced acetylcholine release from SIA neurons, the *cat-2* mutation should have no effect in animals in which acetylcholine is removed from the SIA neurons. We therefore performed SIA neuron-specific RNAi of *cha-1* in a *cat-2* mutant background and found that the aldicarb sensitivity of this strain was not significantly different from that of animals with a wild-type background that were subjected to *cha-1* RNAi. Hence, *cha-1* RNAi did not increase the aldicarb resistance of *cat-2* but rather decreased it to the level of N2 animals subjected to *cha-1* RNAi. This result demonstrates that *cat-2* does not have any effect on aldicarb sensitivity when *cha-1* was knocked down by RNAi using the *ceh-17* promoter and suggest that the dopamine-mediated modulation of aldicarb sensitivity is dependent on acetylcholine in SIA neurons. There seems to be a tendency for RNAi strains to have a slower decline in the number of moving animals later in the assay than did *cat-2* mutants. These strains carry the transgenes as extrachromosomal arrays and it is possible that variability in the copy number of the transgene is causing a portion of RNAi animals to become more aldicarb resistance.

SIA neurons are known to be cholinergic [15] and have been shown to synapse with the head muscles in *C. elegans* [34]. However, the aldicarb assay used here measured whole-body paralysis, and the observed delay in aldicarb-mediated paralysis for the *cat-2* mutant was not limited to the head muscles; their entire body moved for a longer time after exposure to aldicarb compared with wild-type animals. In addition to connecting to the head muscles, SIA neurons possess neuronal processes that extend from the head region to the tail through the sublateral cords [34]. The function of these processes is unknown. However, neural processes in the sublateral cord contain synaptobrevin [35], which plays a role in vesicle secretion, suggesting that acetylcholine can be released from this region of the neuronal processes. SIA neurons account for only four of approximately 100 cholinergic neurons in *C. elegans*, and the muscles that control body movement are controlled mainly by ventral cord cholinergic motor neurons. Nonetheless, the results presented here suggest that reducing acetylcholine release from these four SIA neurons produces a change in aldicarb-mediated paralysis and negates the effect of *cat-2*. We used *ceh-17* promoter to express double-stranded RNA of *cha-1* with the intention to inhibit expression of *cha-1* only in SIA neurons. The cell-type specificity of *ceh-17* promoter was determined by expressing fluorescent proteins under this promoter [12,32]. However, it remains possible that this promoter induces gene expression in other cholinergic neurons in a way that is too weak to be detected with fluorescent proteins. Such leaky expression of double-stranded RNA may be causing knockdown of *cha-1* in other cholinergic neurons. *cha-1* mutants are very uncoordinated, small, and slow growing [33]. The *cha-1* RNAi strains used in this study did not exhibit these phenotypes and therefore are unlikely to have severely reduced *cha-1* expression in many cholinergic neurons. However, a definitive way to address the involvement of SIA neurons in the amine-mediated regulation of acetylcholine release would be to laser ablate SIA neurons of N2 and *cat-2* mutants and to test them for aldicarb sensitivity as this approach does not depend on cell-specific promoters.

Exogenous application of dopamine causes reduced locomotion of *C. elegans* animals through DOP-3 [19,36]. Furthermore, reduced dopamine clearance in the dopamine transporter mutant *dat-1* causes paralysis of animals in liquid [37]. These results suggest that dopamine signaling reduces activity of muscle, which is regulated by acetylcholine signaling. Our finding that the reduced dopamine in *cat-2* mutants causes reduced acetylcholine signaling is somewhat surprising in that dopamine is having an opposite effect on acetylcholine signaling from these previous studies. This difference may be caused by differences in when and

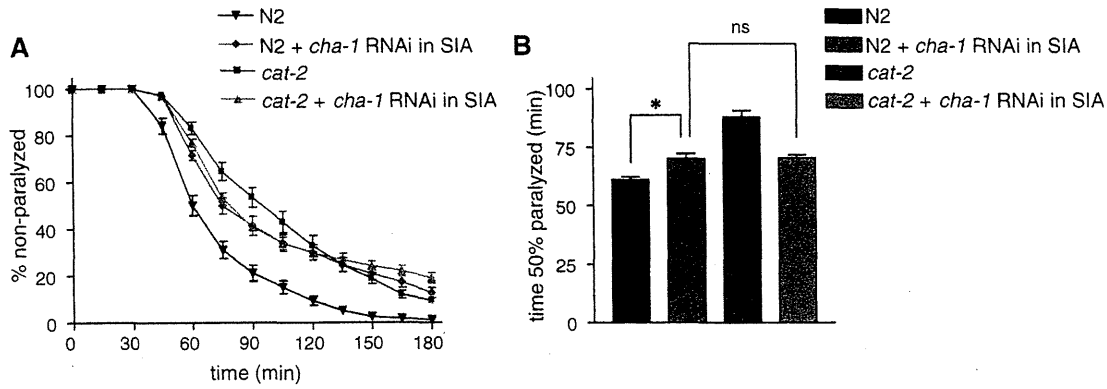

Figure 5. *cha-1* RNAi in wild-type and *cat-2* mutant animals. The choline acetyltransferase gene *cha-1* was specifically knocked down by RNAi in the SIA neurons of wild-type N2 animals or in the *cat-2* mutant. (A) The animals were examined for paralysis on NGM plates containing 1 mM aldicarb. (B) The time required for 50% of the animals to become paralyzed was determined using Prism. *cha-1* RNAi in SIA neurons resulted in increased aldicarb resistance in a wild-type background. The *cat-2* mutation did not significantly alter aldicarb sensitivity when *cha-1* was knocked down in SIA neurons. *P<0.001, ns: P>0.05, by the Tukey-Kramer multiple comparison test. Error bars indicate the SEM.
doi:10.1371/journal.pone.0072578.g005

where dopamine works. Exogenous dopamine and liquid treatment induce acute behavioral changes and exogenously applied dopamine works on the ventral cord motor neurons to control locomotion. On the other hand, it is likely that the effect of dopamine on aldicarb resistance we observed here is a slow response since it depends on a transcription factor CREB and that the SIA neurons play a role in this regulation. Our findings together with the previous reports suggest that dopamine regulates muscle activity through multiple mechanisms.

Conclusions

Studies using several model animals have demonstrated that amine neurotransmitters regulate CREB to induce long-term changes in neuronal activity. In this study, we found that multiple dopamine signaling mutants exhibited increased aldicarb resistance, which is indicative of reduced acetylcholine signaling. Genetic experiments revealed that octopamine and CREB signaling, which is suppressed by dopamine in the presence of food, functions downstream of dopamine and that activation of this signaling pathway reduces acetylcholine release. Cell-specific rescue and knockdown experiments suggested the involvement of SIA neurons for the regulation of acetylcholine signaling by dopamine. The results of this study indicate that the regulation of CREB by amine neurotransmitter signaling modulates neurotransmitter release in *C. elegans*. Our findings will facilitate future studies of the mechanism of the CREB-mediated regulation of neurotransmitter release in the genetically tractable model organism *C. elegans*.

Acknowledgments

We thank Drs. H. Van Tol and J. Culotti for their invaluable support. *cat-2(tm2261)* was isolated by the NBRP. Some strains were provided by the CGC, which is funded by the NIH Office of Research Infrastructure Programs (P40 OD010440).

Author Contributions

Conceived and designed the experiments: SS. Performed the experiments: SS. Analyzed the data: SS SI. Wrote the paper: SS.

References

1. Mayr B, Montminy M (2001) Transcriptional regulation by the phosphorylation-dependent factor CREB. Nat Rev Mol Cell Biol 2: 599–609.
2. Hyman SE (1996) Addiction to cocaine and amphetamine. Neuron 16: 901–904.
3. Mayford M, Kandel ER (1999) Genetic approaches to memory storage. Trends Genet 15: 463–470.
4. Sakamoto K, Karelina K, Obrietan K (2011) CREB: a multifaceted regulator of neuronal plasticity and protection. J Neurochem 116: 1–9.
5. Kimura Y, Corcoran EE, Eto K, Gengyo-Ando K, Muramatsu M, et al. (2002) A CaMK cascade activates CRE-mediated transcription in neurons of *Caenorhabditis elegans*. EMBO rep 3: 962–966.
6. Kauffman AL, Ashraf JM, Corces-Zimmerman MR, Landis JN, Murphy CT (2010) Insulin signaling and dietary restriction differentially influence the decline of learning and memory with age. PLoS Biol 8: e1000372.
7. Nishida Y, Sugi T, Nonomura M, Mori I (2011) Identification of the AFD neuron as the site of action of the CREB protein in *Caenorhabditis elegans* thermotaxis. EMBO Rep 12: 855–862.
8. Timbers TA, Rankin CH (2011) Tap withdrawal circuit interneurons require CREB for long-term habituation in *Caenorhabditis elegans*. Behav Neurosci 125: 560–566.
9. Amano H, Maruyama IN (2011) Aversive olfactory learning and associative long-term memory in *Caenorhabditis elegans*. Learn Mem 18: 654–665.
10. Zubenko GS, Jones ML, Estevez AO, Hughes HB, Estevez M (2009) Identification of a CREB-Dependent Serotonergic Pathway and Neuronal Circuit Regulating Foraging Behavior in *Caenorhabditis elegans*: A Useful Model for Mental Disorders and Their Treatments? Am J Med Genet B Neuropsychiatr Genet 150B: 12–23.
11. Mair W, Morantte I, Rodrigues APC, Manning G, Montminy M, et al. (2011) Lifespan extension induced by AMPK and calcineurin is mediated by CRTC-1 and CREB. Nature 470: 404–408.
12. Suo S, Kimura Y, Van Tol HHM (2006) Starvation induces cAMP response element-binding protein-dependent gene expression through octopamine-Gq signaling in *Caenorhabditis elegans*. J Neurosci 26: 10082–10090.
13. Suo S, Culotti JG, Van Tol HHM (2009) Dopamine counteracts octopamine signalling in a neural circuit mediating food response in *C. elegans*. EMBO J 28: 2437–2448.
14. Roeder T (1999) Octopamine in invertebrates. Prog Neurobiol 59: 533–561.
15. Riddle DL, Blumenthal T, Meyer BJ, Priess JR (1997) *C. elegans* II. 2nd ed. Cold Spring Harbor (NY): Cold Spring Harbor Laboratory Press.
16. Brenner S (1974) The genetics of *Caenorhabditis elegans*. Genetics 77: 71–94.
17. Sulston J, Dew M, Brenner S (1975) Dopaminergic neurons in the nematode *Caenorhabditis elegans*. J Comp Neurol 163: 215–226.
18. Kimura KD, Fujita K, Katsura I (2010) Enhancement of Odor Avoidance Regulated by Dopamine Signaling in *Caenorhabditis elegans*. J Neurosci 30: 16365–16375.
19. Chase DL, Pepper JS, Koelle MR (2004) Mechanism of extrasynaptic dopamine signaling in *Caenorhabditis elegans*. Nature Neuroscience 7: 1096–1103.
20. Mahoney TR, Luo S, Nonet ML (2006) Analysis of synaptic transmission in *Caenorhabditis elegans* using an aldicarb-sensitivity assay. Nature Protocols 1: 1772–1777.
21. Murakami M, Koga M, Ohshima Y (2001) DAF-7/TGF-β expression required for the normal larval development in *C. elegans* is controlled by a presumed guanylyl cyclase DAF-11. Mechanisms of Development 109: 27–35.
22. Esposito G, Di Schiavi E, Bergamasco C, Bazzicalupo P (2007) Efficient and cell specific knock-down of gene function in targeted *C. elegans* neurons. Gene 395: 170–176.
23. Tenor JL, Aballay A (2008) A conserved Toll-like receptor is required for *Caenorhabditis elegans* innate immunity. EMBO Rep 9: 103–109.
24. Lints R, Emmons SW (1999) Patterning of dopaminergic neurotransmitter identity among *Caenorhabditis elegans* ray sensory neurons by a TGFβ family signaling pathway and a Hox gene. Development 126: 5819–5831.
25. Suo S, Sasagawa N, Ishiura S (2003) Cloning and characterization of a *Caenorhabditis elegans* D2-like dopamine receptor. J Neurochem 86: 869–878.
26. Sugiura M, Fuke S, Suo S, Sasagawa N, Van Tol HHM, et al. (2005) Characterization of a novel D2-like dopamine receptor with a truncated splice variant and a D1-like dopamine receptor unique to invertebrates from *Caenorhabditis elegans*. J Neurochem 94: 1146–1157.
27. Allen AT, Maher KN, Wani KA, Betts KE, Chase DL (2011) Coexpressed D1- and D2-Like Dopamine Receptors Antagonistically Modulate Acetylcholine Release in *Caenorhabditis elegans*. Genetics 188: 579–590.
28. Herman RK, Kari CK (1985) Muscle-specific expression of a gene affecting acetylcholinesterase in the nematode *Caenorhabditis elegans*. Cell 40: 509–514.
29. Sawin ER, Ranganathan R, Horvitz HR (2000) *C. elegans* Locomotory Rate Is Modulated by the Environment through a Dopaminergic Pathway and by Experience through a Serotonergic Pathway. Neuron 26: 619–631.
30. Alkema MJ, Hunter-Ensor M, Ringstad N, Horvitz HR (2005) Tyramine Functions Independently of Octopamine in the *Caenorhabditis elegans* Nervous System. Neuron 46: 247–260.
31. Lewis JA, Elmer JS, Skimming J, McLafferty S, Fleming J, et al. (1987) Cholinergic receptor mutants of the nematode *Caenorhabditis elegans*. J Neurosci 7: 3059–3071.
32. Pujol N, Torregrossa P, Ewbank JJ, Brunet JF (2000) The homeodomain protein CePHOX2/CEH-17 controls antero-posterior axonal growth in *C. elegans*. Development 127: 3361–3371.
33. Rand JB, Russell RL (1984) Choline acetyltransferase-deficient mutants of the nematode *Caenorhabditis elegans*. Genetics 106: 227–248.
34. White JG, Southgate E, Thomson JN, Brenner S (1986) The structure of the nervous system of the nematode *Caenorhabditis elegans*. Philos Trans R Soc Lond, B, Biol Sci 314: 1–340.
35. Nonet ML (1999) Visualization of synaptic specializations in live *C. elegans* with synaptic vesicle protein-GFP fusions. J Neurosci Methods 89: 33–40.
36. Schafer WR, Kenyon CJ (1995) A calcium-channel homologue required for adaptation to dopamine and serotonin in *Caenorhabditis elegans*. Nature 375: 73–78.
37. McDonald PW, Hardie SL, Jessen TN, Carvelli L, Matthies DS, et al. (2007) Vigorous Motor Activity in *Caenorhabditis elegans* Requires Efficient Clearance of Dopamine Mediated by Synaptic Localization of the Dopamine Transporter DAT-1. J Neurosci 27: 14216–14227.

Original Article

DOI: 10.5582/bst.2013.v7.6.270

A high-salinity solution with calcium chloride enables RNase-free, easy plasmid isolation within 55 minutes

Noboru Sasagawa[1,*], Michinori Koebis[2], Yoji Yonemura[2], Hiroaki Mitsuhashi[3], Shoichi Ishiura[2]

[1] *Department of Applied Biochemistry, School of Engineering, Tokai University, Kanagawa, Japan;*
[2] *Department of Life Sciences, Graduate School of Arts and Sciences, University of Tokyo, Tokyo, Japan;*
[3] *Life Science Network, University of Tokyo, Tokyo, Japan.*

Summary **We dramatically improved a plasmid-isolation protocol based on the popular alkaline-sodium dodecyl sulfate plasmid isolation method. Our modified method provides significant time and cost savings. We used a modified solution during the neutralization step, which allowed us to skip several subsequent handling steps, saving a great amount of time. The plasmids purified by this method were of high quality, and the optical density ratio 260 and 280 was approximately 1.8. Plasmid DNA isolated by our method was of sufficient quality to perform subsequent restriction enzyme cuts and other downstream experiments, including budding yeast transformation, cultured cell transfection, and *Caenorhabditis elegans* injection experiments.**

Keywords: Plasmid isolation, calcium chloride, polyethylene glycol, RNase-free

1. Introduction

Plasmid isolation from *Escherichia coli* is an indispensable step in most routine laboratory experiments for molecular biology, biochemistry, and cell biology. There are several published plasmid-isolation methods (*1-8*). Among them, the alkaline-sodium dodecyl sulfate (SDS) method (*1*) is the most popular procedure for purifying plasmid DNA. In this method, the DNA denaturation step (using Solution II) and neutralization step (using Solution III) are very effective and sophisticated techniques for separating plasmid DNA from *E. coli* genomic DNA. Moreover, insoluble cellular debris, including proteins, is separated together with genomic DNA from plasmids. One of the difficulties of this popular method is that a huge amount of RNA is collected along with the plasmid DNA. Therefore, RNase is always required to remove unwanted RNA from the plasmid solution. Then a hazardous organic solvent (phenol/chloroform) is added to inactivate and remove the RNase protein. This process requires several additional steps and extra time.

**Address correspondence to:*
Dr. Noboru Sasagawa, Department of Applied Biochemistry, School of Engineering, Tokai University, Kanagawa 259-1292, Japan.
E-mail: noboru.sasagawa@tokai-u.jp

Many commercial kits are available for plasmid isolation. Two major kits with different principles are widely used. One is based on an anion-exchange resin (*9*). Plasmid DNA is adsorbed onto the resin by the negative charge of DNA and then eluted by adding a high-salinity solution. Another method employs a silica membrane with chaotropic solutions (*10,11*). Under chaotropic conditions, nucleic acids are adsorbed onto silica particles and eluted using pure water. In both major commercial kits, the principle of separating plasmid DNA from bacterial genomic DNA is still based on the popular alkaline-SDS method. Moreover, both kits require RNase to digest unwanted RNA. Therefore, a large amount of RNase is added to the kit solution. These kits are very easy to use, but rather expensive. Thus, another time- and cost-saving protocol for high-quality and high-quantity plasmid isolation is needed for everyday experiments in the laboratory. Furthermore, RNase is widely known as a robust, stable protein. RNase protein contamination results in the degradation of RNA in the laboratory and disrupts RNA experiments. It is best not to use RNase protein in laboratories that handle RNA molecules.

Calcium chloride ($CaCl_2$) is an effective reagent that selectively removes RNA from a mixture of DNA and RNA (*12,13*). That is, RNA can be precipitated by centrifugation in the presence of $CaCl_2$ (RNase is not needed). However, this requires several centrifugation

steps and takes quite a long time. Hence, we established a modified plasmid purification method using $CaCl_2$ (called the Super Sol III method or Sasagawa method) that is based on standard alkaline-SDS isolation but is much easier and less time consuming. Our method eliminates several steps, allowing us to isolate plasmid DNA in much less time, and the total isolation time is around 55 min.

2. Materials and Methods

2.1. *E. coli, liquid medium, and plasmid DNA*

We used *E. coli* JM109 or XL-1 blue, which we routinely use for cloning experiments. Bacteria were grown in LB medium supplemented with ampicillin (final concentration, 50 μL/mL). *E. coli* was incubated in 15-50-mL tubes with 5-10 mL LB medium in a shaking air incubator. The plasmids pBluescript and pUC118, and their derivatives, were also tested.

2.2. *Reagents and equipment*

For all of our experiments, the purest grade reagents available were purchased from Wako Pure Chemical Industries (Osaka, Japan) or Nacalai Tesque (Kyoto, Japan). Solutions I and II were prepared according to a standard protocol (*14*). We purchased restriction enzymes from Takara-Bio (Shiga, Japan) and/or Toyobo (Osaka, Japan) to cut plasmid DNA. Sample quality and quantity were determined using a NanoDrop 2000 (Thermo Fisher Scientific, Yokohama, Japan). A Narishige micromanipulator (Tokyo, Japan) was used to inject plasmid into *C. elegans*.

2.3. *Super Sol III solution*

The modified Solution III (Super sol III or Sol III-Ca) consisted of 1 mL Solution III (*14*), 1 mL 5 M $CaCl_2$, and 0.5 mL H_2O. A warming step to dissolve the solution might be needed (*i.e.*, 37°C or above).

2.4. *Handmade filtration column*

We made a filtration column as follows (Figure 1). The bottom of a 5-mL polystyrene round-bottom tube (*e.g.*, Falcon 352058) was drilled using a heated ice pick to create a pinhole (Figure 1a). A polypropylene centrifuge tube (15 mL) was used for sample collection. We made a hole in a 15-mL screw cap tube using a cork borer (#6, Φ12 mm). The round-bottom tube was inserted through the cap hole, and the top of the round-bottom tube was taped with electrical tape as a stopper (Figure 1b). A piece of tissue paper was pushed firmly into a 5-mL polystyrene round-bottom tube (Figure 1c). Before use, 5 mL H_2O was applied and the filter was washed using centrifugation. After centrifugation, filtered H_2O was discarded.

2.5. *Budding yeast, cultured cells, and C. elegans*

The budding yeast *Saccharomyces cerevisiae* strain PJ69-4A was used for transformation. A derivative of plasmid p426ADH (*15*) was transformed into the yeast using URA3 as a selectable marker. A pEGFP plasmid was transfected into HeLa cells as a model of mammalian cell transfection. *C. elegans* (N2 strain) were injected with plasmids pRF4, in which a mutated collagen gene is coded.

3. Results

3.1. *Removal of high-molecular-weight RNA in a single step*

Our first challenge was to modify Solution III by adding $CaCl_2$. We named the new mixture Super Sol III. We tested it and found that it neutralized as well as traditional Solution III. Moreover, it greatly reduced the amount of RNA in the cleared lysate. Higher molecular weight RNA precipitates out with protein and genomic DNA. Only small RNAs, such as tRNA, seem to remain in the lysate (Figure 2, lane 3).

Centrifugation was thought to be necessary to precipitate RNA in the presence of $CaCl_2$. However, surprisingly, we found that centrifugation was not absolutely necessary to remove high-molecular-weight RNA. To test the effect of Super Sol III on RNA removal from the lysate, we first filtered the neutralized sample solution, which contained a large amount of debris, without using centrifugation. We then added 2-propanol to the filtered lysate and centrifuged the

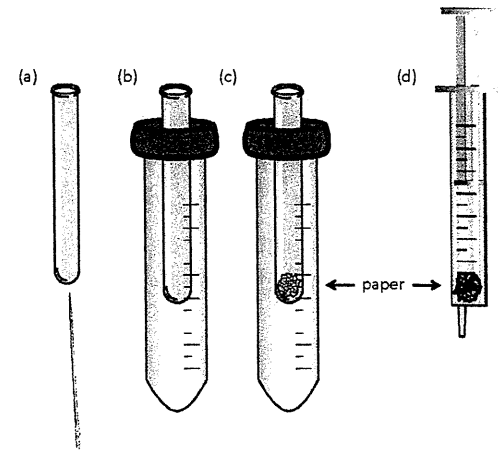

Figure 1. A handmade filtration column. **(a)** A hole was made in the bottom of a round-bottom 5-mL polystyrene tube using a heated needle. **(b)** A hole was made in the top of a 15-mL tube screw cap, and a 5-mL tube **(a)** was inserted through the hole. The top of the round-bottom tube was taped with electrical tape as a stopper. **(c)** A piece of tissue paper was pushed into a 5-mL polystyrene round-bottom tube. **(d)** A 2.5-10-mL disposable syringe with tissue paper could also be used as a handmade filter in this experiment.

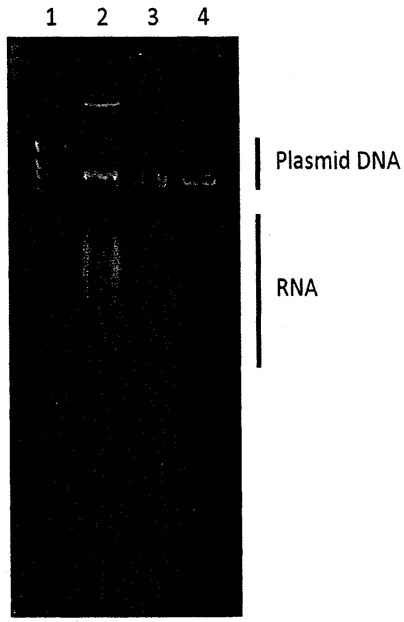

Figure 2. Effect of RNA removal by $CaCl_2$, which is premixed into Solution III. Lane 1: molecular weight marker. Lane 2: negative control (standard alkali-SDS plasmid purification without RNase). Lane 3: a solution neutralized by Super Sol III was centrifuged, and then 2-propanol precipitation was performed. Lane 4: a solution neutralized by Super Sol III was filtered without centrifugation, and then 2-propanol precipitation was performed.

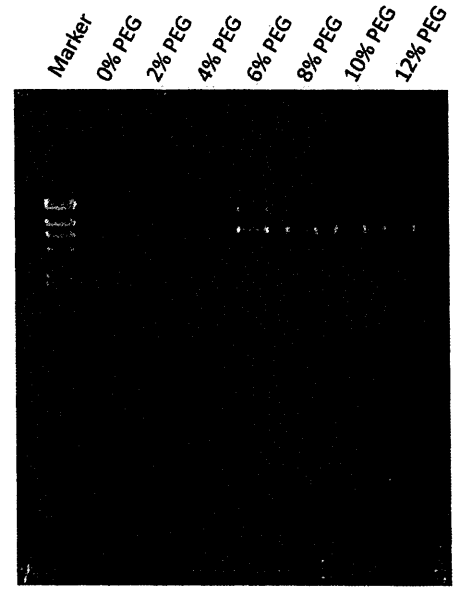

Figure 3. A combination of Super Sol III and polyethylene glycol precipitation. Lane 1: molecular weight marker. Lanes 2–8 represent various final concentrations of polyethylene glycol (PEG) during the plasmid precipitation step. Lane 2: 0% PEG. Lane 3: 2% PEG. Lane 4: 4% PEG. Lane 5: 6% PEG. Lane 6: 8% PEG. Lane 7: 10% PEG. Lane 8: 12% PEG.

sample to precipitate nucleic acids. This procedure resulted in the recovery of plasmid DNA and a small amount of RNA (Figure 2, lane 4). These results indicate that a large amount of RNA became insoluble, and was removed with insoluble proteins and debris as well as genomic DNA during the filtration step.

3.2. *A combination of Super Sol III and polyethylene glycol precipitation*

Based on the above results, we further improved the protocol by adding polyethylene glycol directly to the filtered lysate to precipitate plasmid DNA. Polyethylene glycol precipitates plasmid DNA, but not small-molecular-weight RNA (*16,17*). We added polyethylene glycol to a final concentration of 0-12% to filtered lysate and centrifuged the sample to precipitate plasmid DNA. Pure plasmid DNA without unwanted RNA was obtained. Even small-molecular-weight RNA disappeared from the sample (Figure 3). A final concentration of 6-12% polyethylene glycol produced good results. Therefore, we decided to precipitate plasmid DNA to a final concentration of 8% polyethylene glycol by adding 32% polyethylene glycol solution. Both polyethylene glycol #4,000 and #6,000 worked well for precipitating clear plasmid DNA (data not shown).

Prior to polyethylene glycol precipitation, the debris (*i.e.*, insoluble proteins and genomic DNA) should be completely removed from the lysate. For this purpose, we made a handmade filtration column (Figure 1). Based on these results, we established our complete plasmid purification protocol (Figure 4).

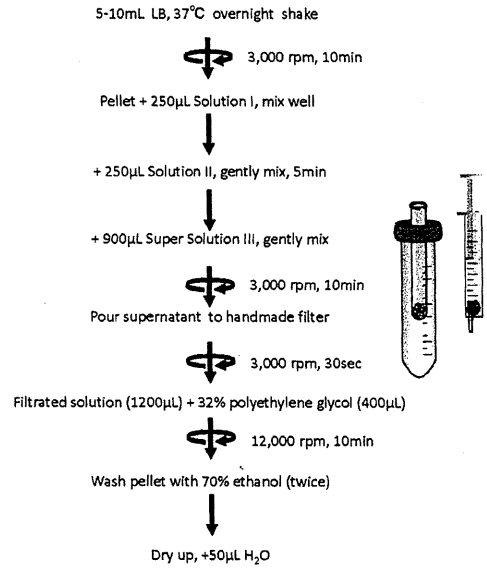

Figure 4. The complete 55-min protocol established in this study.

3.3. *Quality and quantity check of plasmid DNA by spectrophotometer*

We checked the quality of plasmid DNA purified by our Super Sol III method. As shown in Table 1, we obtained very high quality plasmid DNA. The optical

Table 1. Spectrophotometric DNA quality and quantity check

	A_{260}	Conc.(ng/μL)	Total plasmid (μg)	A_{260}/A_{280}
Average	3.58	179	8.95	1.85
S.D	1.81	91	4.54	0.04

Data are presented as average ± S.D.

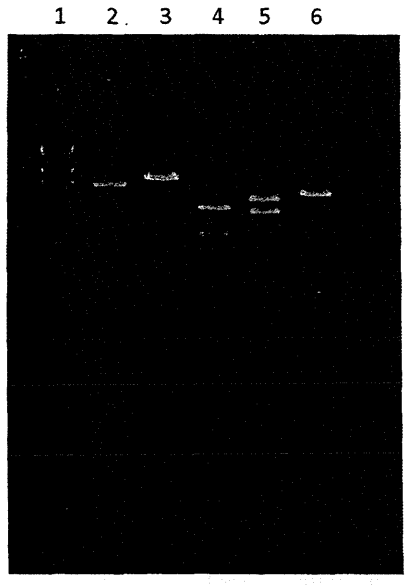

Figure 5. Restriction enzyme check. Lane 1: molecular weight marker. Lane 2: uncut plasmid DNA. Lane 3: *Kpn* I cut (Low-salt buffer). Lane 4: *Hind* III cut (Medium-salt buffer). Lane 5: *Eco* R I cut (High-salt buffer). Lane 6: *Bam* H I cut (High-salt buffer with potassium).

density ratio at 260 and 280 (A_{260}/A_{280}) was around 1.8, indicating that there was no protein contamination in the isolated plasmid. The quantity of plasmid DNA was almost 1 μg/mL in LB medium, which is sufficient for downstream experiments. We found that both handmade-columns and syringe filters have good qualities (Table 1).

3.4. *Restriction enzyme check*

The quality of purified plasmid DNA was also checked by using restriction enzymes. A purified plasmid was cut with *Eco* R I (High-salt buffer), *Bam* H I (High-salt buffer with potassium), *Hind* III (Medium-salt buffer), and *Kpn* I (Low-salt buffer). All of these enzymes successfully cut plasmid DNA (Figure 5).

3.5. *Injection into C. elegans*

To check the quality of the purified plasmid, we injected plasmids into *C. elegans* following a previous study (*18*). Generally, we obtain F1 transformants in the injection experiments, but the F2 transformant (*i.e.* stable transformant) appears only when the transgene is provided in the F1 germline. That is, we can conclude the stable transformation experiment was successful

Table 2. Results of DNA injection into *C. elegans*

Injected worm	9
F1 transformant	6
F2 transformant	3

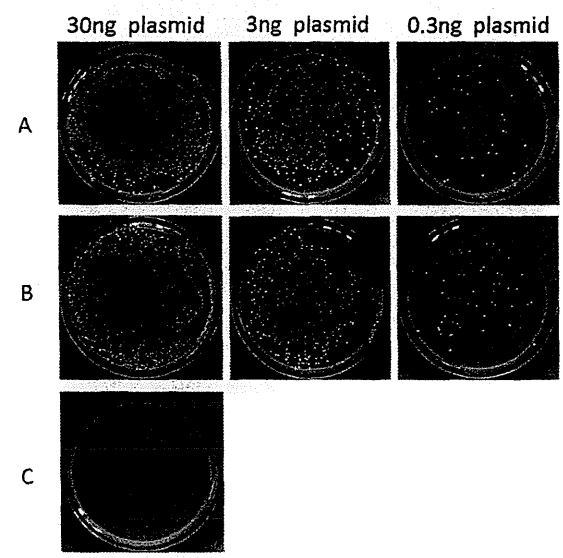

Figure 6. Results of yeast transformation. In total 30 ng, 3 ng, and 0.3 ng plasmid per plate were transformed into the budding yeast. **(A)**, plasmid DNA isolated by our protocol. **(B)**, plasmid DNA isolated by a standard silica membrane kit (positive control). **(C)**, no plasmid DNA (negative control).

only when we obtained F2 transformants. We injected plasmid DNA from our method into nine worms, and obtained six F1 transformants. And then, one of the F1 transformants had F2 transformants, indicating that our injection experiments were successful using the plasmid purified by our method (Table 2).

3.6. *Yeast transformation*

We performed yeast transformation in *S. cerevisiae* to determine plasmid DNA quality. A derivative of plasmid p426ADH (*15*) was purified using our plasmid isolation method, and then transformed into *S. cerevisiae* with a standard lithium chloride protocol (*19*). As shown in Figure 6, transformation was efficient with our plasmid, and was similar to the plasmid transformation efficiency achieved when using a Sigma commercial kit (*10*). Transformation efficiency was calculated as colony forming units per 1 μg plasmid (cfu/μg). According to this calculation, the efficiency of our system was 1.8×10^5 cfu/μg, while the efficiency using the Sigma kit was 2.5×10^5 cfu/μg. Generally, around 10^5 cfu/μg is an acceptable result.

3.7. *Transfection into cultured cells*

Our plasmid-isolation method also provided plasmids of sufficient quality for transfection into cultured cells.

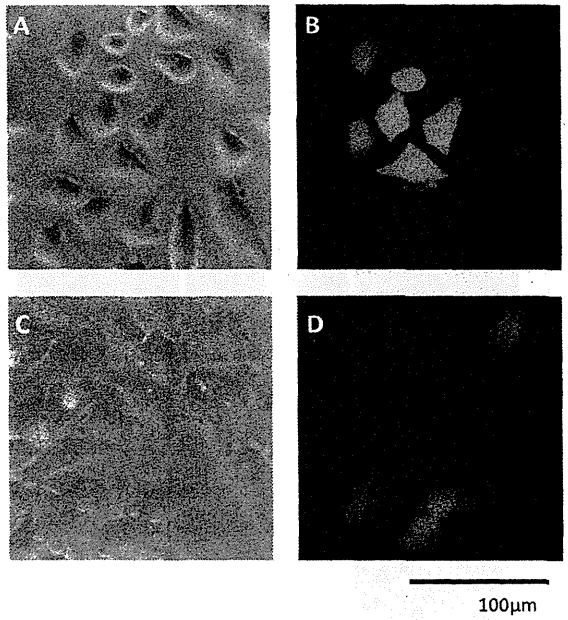

Figure 7. Result of cultured cell transfection. Upper panels **(A, B)** are cells transfected using a plasmid described in this manuscript, and lower panels **(C, D)** are cells using a commercial kit. **(A)** and **(C)**, phase-contrast image; **(B)** and **(D)**, EGFP fluorescence detection.

Using the standard Fugene 6.0 (Promega) protocol (*20*), 0.5 μg pEGFP plasmid was transfected into cells seeded in a 20-mm dish. As shown in Figure 7, we successfully observed EGFP fluorescence in HeLa cells. This indicates that plasmid DNA isolated by our method is of sufficient quality for use in cell transfection. We counted cells in microscopic images and calculated transfection efficiencies. The transfection efficiency of our plasmid isolation method was 20%, whereas the efficiency was 50% when we transfected a plasmid with a Sigma kit.

4. Discussion

The advantage of the traditional alkaline-SDS method is that chromosomal *E. coli* DNA is removed, along with insoluble debris, by several simple steps, leaving plasmid DNA in the cleared lysate. The basic steps of this traditional method include cell lysis and protein/DNA denaturation by the alkaline solution (Sol II) and a sudden pH change to neutrality by neutralization buffer (Sol III). This sudden pH change is essential to transform genomic DNA and proteins into insoluble debris.

The difficulty of this method lies in separating RNA from the cleared lysate; RNA and plasmid DNA react similarly to pH changes. Therefore, an RNA-removal step using RNase is always needed, which requires additional processes such as phenol/chloroform extraction.

Our new plasmid-purification protocol greatly improved on previous methods in two ways. First, we modified Solution III (into Super Sol III) by adding calcium chloride to directly remove a large amount of RNA during the neutralization step. This allowed us to purify plasmid high quality DNA in fewer steps. It also did not require RNase incubation or a hazardous phenol/chloroform extraction step. Our modified Solution III removed unwanted RNA in the neutralization step without centrifugation. A small amount of RNA still remained in the cleared lysate, which was easily removed by simple polyethylene glycol precipitation. Second, we added a filtration step. Unlike an anion-exchange column and/or a silica membrane column, our column simply filtered and separated insoluble debris. In our protocol (Figure 4), centrifugation was performed before filtration not to precipitate RNA but simply to reduce debris. Use of a commercial filter and/or gel filtration resin (such as Sephadex) may lead to a much better result, although our handmade column was sufficient for our experiments. The syringe filter was easier to handle, although the total quantity was better in the handmade-column than the syringe (Table 1). This might be due to the dead volume of the syringe filter. The syringe filter is still applicable because the plasmid purified using the syringe filter had a quality good enough for downstream experiments. In our manuscript, Figure 2, Table 1 (in part) and Table 2 were data using the syringe filter, and others were from the handmade-column. We tested both filters and concluded that they worked well in our daily experiments (data not shown).

Too large of an amount of *E. coli* at the start (*i.e.* too much *E. coli* cells for reagent volumes) results in insoluble impurities in the final plasmid solution. It is important to keep a volume balance between solutions and *E. coli*. In large-scale experiments, simply dividing *E. coli* samples into several test tubes will give a good result. An option for scaling up is to use a 50-mL polypropylene centrifuge tubes and 15-mL polystyrene round-bottom tubes for the handmade-column, instead of the tubes indicated in Figure 1. We checked and confirmed that this scaled-up protocol worked well up to 50-mL LB medium (data not shown).

Generally, super-high-quality plasmid DNA is required for injection into *C. elegans* or transfection into cultured cells. Our data strongly suggests that plasmid DNA isolated by our protocol is of high enough quality for use in biochemical reactions and transformations. A Sigma commercial kit showed better transfection efficiency for cultured cells than our method, but it is very surprising that we can prepare a transfection-grade plasmid by such a simple protocol as described in this manuscript. This commercial kit describes that up to 15 μg of plasmid DNA can be purified from 1-5 mL of *E. coli* culture (*10*), which is a better quantity than our method. Nevertheless, our method has good quality and quantity for downstream experiments (Table 1). Besides, our method has significant advantages that we

do not need RNase, any special reagents or equipment. The column and syringe are recyclable, so that we do not need to take these costs into account.

Acknowledgements

We thank Ryo Kinoshita for valuable advice.

References

1. Birnboim HC, Doly J. A rapid alkaline extraction procedure for screening recombinant plasmid DNA. Nuc Acid Res. 1979; 7:1513-1523.
2. Holmes DS, Quigley M. A rapid boiling method for the preparation of bacterial plasmids. Anal Biochem. 1981; 114:193-197.
3. Marko MA, Chipperfield R, Birnboim HC. A procedure for the large scale isolation of highly purified plasmid DNA using alkaline extraction and binding to glass powder. Anal Biochem. 1982; 121:382-387.
4. Boom R, Sol CJ, Salimans MM, Jansen CL, Wertheim-van Dillen PM, van der Noordaa J. Rapid and simple method for purification of nucleic acids. J Clin Microbiol. 1990; 28:495-503.
5. Tiainen P, Gustavsson PE, Månsson MO, Larsson PO. Plasmid purification using non-porous anion-exchange silica fibres. J Chromatogr A. 2007; 1149:158-168.
6. Grunwald AG, Shields MS. Plasmid purification using membrane-based anion-exchange chromatography. Anal Biochem. 2001; 296:138-141.
7. Elkin CJ, Richardson PM, Fourcade HM, Hammon NM, Pollard MJ, Predki PF, Glavina T, Hawkins TL. High-throughput plasmid purification for capillary sequencing. Genome Res. 2001; 11:1269-1274.
8. Lakshmi R, Baskar V, Ranga U. Extraction of superior-quality plasmid DNA by a combination of modified alkaline lysis and silica matrix. Anal Biochem. 1999; 272:109-112.
9. QIAGEN Plasmid Purification Handbook, QIAGEN, 2012.
10. GenElute™ Plasmid Miniprep Kit, Sigma-Aldrich, 2010.
11. Technical Bulletin #TB117, Promega, 2011.
12. Eon-Duval A, Gumbs K, Ellett C. Precipitation of RNA impurities with high salt in a plasmid DNA purification process: Use of experimental design to determine reaction conditions. Biotechnol Bioeng. 2003; 83:544-553.
13. Sauer ML, Kollars B, Geraets R, Sutton F. Sequential $CaCl_2$, polyethylene glycol precipitation for RNase-free plasmid DNA isolation. Anal Biochem. 2008; 380:310-314.
14. Sambrook J, Russell DW. Molecular Cloning: A Laboratory Manual. Cold Spring Harbor Laboratory Press, Woodbury, NY, USA, 2001.
15. Futai E, Yagishita S, Ishiura S. Nicastrin is dispensable for γ-secretase protease activity in the presence of specific presenilin mutations. J Biol Chem. 2009; 284:13013-13022.
16. Paithankar KR, Prasad KS. Precipitation of DNA by polyethylene glycol and ethanol. Nuc Acid Res. 1991; 19:1346.
17. Hartley JL, Bowen H. PEG precipitation for selective removal of small DNA fragments. Focus. 1996; 18:27.
18. Mello CC, Kramer JM, Stinchcomb D, Ambros V. Efficient gene transfer in *C. elegans*: Extrachromosomal maintenance and integration of transforming sequences. EMBO J. 1991; 10:3959-3970.
19. Yeast protocol handbook, Clomtech, PR973283, 2009.
20. Technical manual #TM350, Promega, 2011.

(Received October 5, 2013; Revised October 30, 2013; Accepted November 3, 2013)

＜シンポジウム　(2)-7-3＞筋疾患研究最前線

筋強直性ジストロフィー

石浦　章一[1)]　小穴　康介[1)]　古戎　道典[1)]

要旨：現在まで，筋強直性ジストロフィーの完璧な治療法はない．私たちは，ミオトニアを指標とする塩化物イオンチャネルのスプライシングの正常化に関して，モデル動物をもちいて２つのアプローチをおこない，効果をしらべた．１つはアンチセンス法で，バブルリポソームという新しい方法で効率的に骨格筋にアンチセンスを導入し，ミオトニアを正常化することに成功した．もう１つは低分子化合物で，塩化物イオンチャネルのスプライシングを正常化する物質マニュマイシンＡを同定し，効果を明らかにした．

（臨床神経 2013;53:1109-1111）
Key words：筋強直性ジストロフィー，スプライシング，塩化物イオンチャネル，ミオトニア，治療

はじめに

筋強直性ジストロフィー（DM）は成人型の筋ジストロフィーで，筋萎縮のみならず，筋強直，精巣萎縮，白内障，耐糖能異常などを特徴とする全身性疾患で[1)2)]，我が国の発病率は約８千人に１人である．また，家系には重篤な症状の先天型がみられることがある．DMのほとんどを占める１型（DM1）の責任遺伝子は第19染色体にあるDMPKで，その3'非翻訳領域にあるCTGリピートの伸長が病気の直接の原因である．また筋強直性ジストロフィー２型（DM2）も発見されたが，これは第３染色体にあるZNF9（CNBP）遺伝子中のイントロン１にあるCCTGリピートの伸長であることが明らかになった．その後，DMPK mRNAが核にfociを作ることが判明し，そこにRNA結合タンパク質が集積していることがわかってきた．また，伸長したリピートだけを発現させたマウスでもヒトと同じ症状がみられたり[3)]，DMPKのヘテロでは症状がまったくみとめられないことから，RNAリピートが発症にかかわっているという説が有力になってきた．本研究では，ミオトニアの原因である塩化物イオンチャネル（*Clcn1*）遺伝子のスプライシングを正常化することを目的に研究をおこなった．

アンチセンスオリゴによるスプライシングの正常化

以下の実験には，HSA^{LR}マウスをもちいた．このマウスは骨格筋アクチンプロモーターの下流に約CTG200リピートをつないだトランスジェニックマウスで，ロチェスター大学のC.A. Thornton教授から供与されたものである．

Fig. 1Aにはマウス*Clcn1*遺伝子のエキソン６～７の模式図を示す．まず，エキソン6，7A，7をふくむミニ遺伝子を作成し，COS-7をもちいた培養細胞系でエキソン7Aをスキップする正常型スプライシングの割合を高めるアンチセンス配列を検討した．その結果，エキソン7Aの5'側1-25のアンチセンスがもっとも効率よくエキソン7Aをスキップさせることがわかった．そこで次に，1-25モルフォリノオリゴ20 μgを６週令のHSA^{LR}マウスの前脛骨筋（TA）に筋注した．このとき，モルフォリノは30 μlのバブルリポソームに懸濁してもちいた．注射後すぐに超音波を患部に与え，試薬の筋への浸透を図った．この工程を１週間おきに３回おこない，最後の照射から３週間後に筋電図を測定し，その後，筋を採取してスプライシングアッセイをおこなった．

Fig. 1B左はスプライシングの結果である．これは筋からmRNAを抽出しcDNAにしたあと，PCRによってしらべたもので，上のバンドがエキソン7Aをふくむ異常型，下のバンドがエキソン7Aをスキップした正常型である．モルフォリノ処理した筋（PMO）では異常型が減少していることがわかる．それを定量化したのがFig. 1B右の図である．

次に，筋電図によりミオトニアが改善されたかどうかについて検討をおこなった．Fig. 1C左は実測図で，HSA^{LR}マウスの片方の足に生理食塩水を，もう片方の足にモルフォリノオリゴ（PMO）を導入したものである．この結果から明らかなように，PMO処理によってミオトニアが減弱したことがわかる．Fig. 1C右はミオトニア量を定量化したもので，単位時間当たりの積分量で表した[4)]．

以上の結果から，新しく調製したアンチセンスオリゴをバブルリポソームと共に投与して超音波処理することにより，筋へアンチセンスが効率よく取り込まれ，ミオトニア症状を改善することができることがわかった．しかし，スプライシングを完全に正常化することはできず，ミオトニアも少し残ることから，投与の最適化にはもう少し時間がかかることがわかった．

[1)] 東京大学大学院総合文化研究科〔〒153-8902　東京都目黒区駒場３丁目8-1〕
（受付日：2013年５月30日）

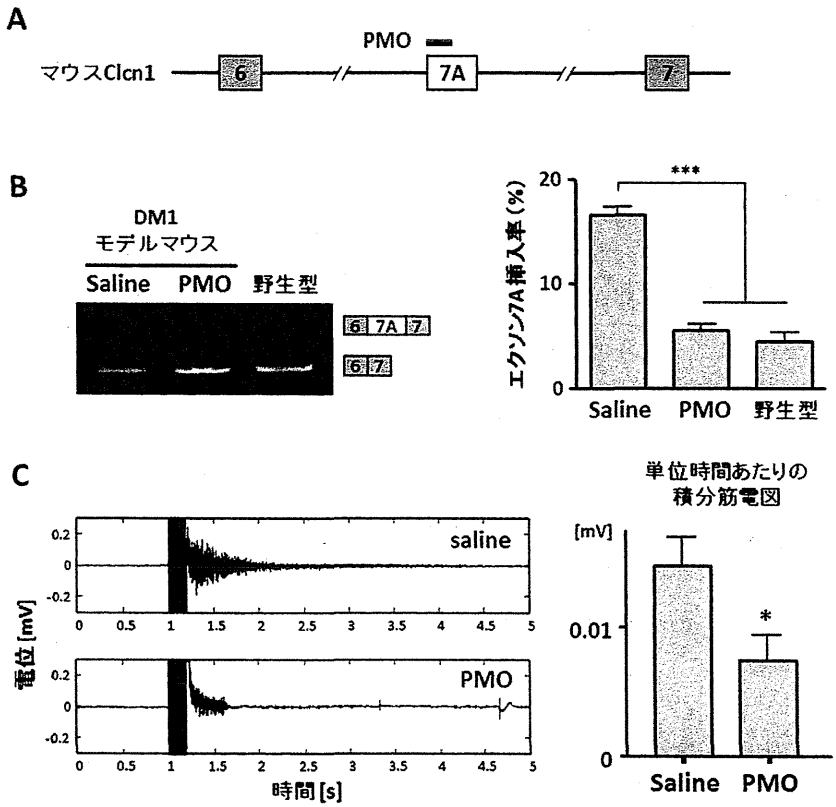

Fig. 1　アンチセンスによるミオトニアの軽減.

低分子化合物によるスプライシングの正常化

私たちは筋への浸透性が高い低分子化合物によってスプライシングを正常化することも試みた. Fig. 2Aには, そのスリーニング手法を示す. まずFig. 1のミニ遺伝子の後方にルシフェラーゼ遺伝子をつないだコンストラクトを作った. マウスC2C12細胞にこのミニ遺伝子を導入して, 正常にスプライシングがおこったばあいには（エキソン7Aが抜ける）ルシフェラーゼが発現し, 異常スプライシングがおこったばあいには途中で停止コドンが入るようにしてルシフェラーゼが発現しないように工夫した. MBNL1のようなエキソン7Aをスキップさせるようなスプライシング因子が存在すると正常スプライシングがおこるが, MBNL1がないと異常の方に傾く. この系によって400種類以上の化合物を試した結果, Fig. 2Cに示すマニュマイシンAという化合物がヒットした[5].

Fig. 2BのようにマニュマイシンAは確かにCTG480リピートの存在下で, 正常スプライシングを促進した. そこで, マニュマイシンAを先ほどのHSA^{LR}マウスのTA筋に3 μg投与し, 5日後に筋肉を回収してスプライシングをみたのがFig. 2Dである. 対照（反対足）には0.1% DMSOを同量投与した. Fig. 2Dの定量結果から, マニュマイシンAは実際のマウス筋においてもスプライシングを正常化することがわかった.

興味深いことに, このマウスClcn1遺伝子のスプライシング正常化にはH-Rasが関与していることがわかった（Fig. 2E）. マニュマイシンAはファルネシル化の阻害剤である. そこで, ファルネシル化されることで有名なRasファミリーをsiRNAによってノックダウンしたところ, H-Rasをノックダウンしたときにマウス*Clcn1*遺伝子のスプライシングが正常化することがわかった. H-Ras以外のRasはファルネシル化の他にゲラニルゲラニル化を受けることが知られている. マニュマイシンAはファルネシル化特異的な阻害剤であるため, マウス*Clcn1*遺伝子のスプライシングにはH-Rasが関係している可能性が示唆された.

おわりに

本研究で明らかになったアンチセンス配列は, エキソン7aの最初の部分であり, ここはMBNL1応答配列と考えられているところである[6]. 私たちが対照に選んだのは, アンチセンス法をはじめてモデルマウスに適用したRochester大学のC.A. Thornton教授が作った配列[7]だが, 比較検討の結果, 今回私たちが新しく同定した配列をもちいたばあいに最大限のスプライシング正常化がみとめられた. また, アンチセンスの導入にバブルリポソームをもちいたのも新規な知見であり, 今後は効率的投与法としてもちいられるであろう.

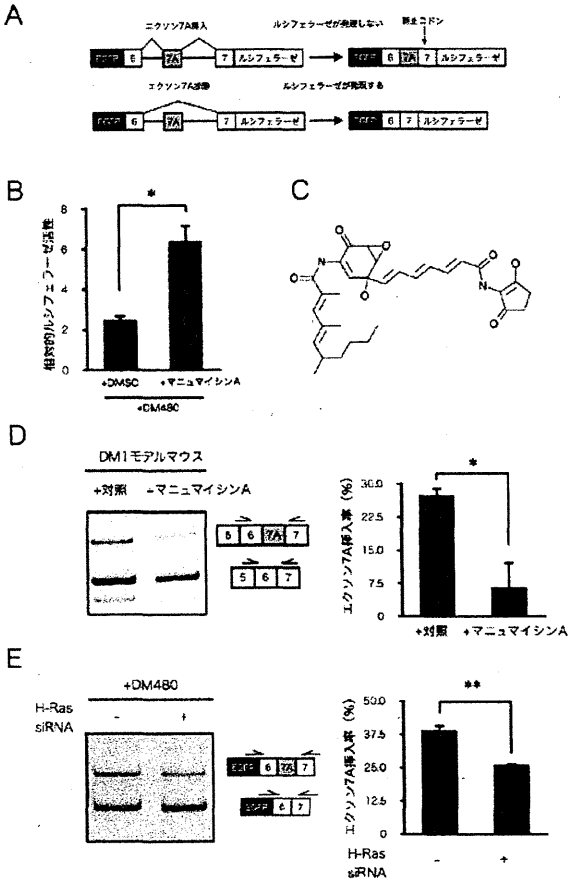

Fig. 2　マニュマイシンによるスプライシングの正常化.

しかしながら効果は限定的で，もう少し効率の良いものが求められる．マニュマイシンAはアンチセンスを補完するものであり，今後，投与法が大きな問題になるものと思われる．もっと重要なのは，DM患者のQOLに大切な筋力低下をどう改善するかという点であり，これについてはほとんど知見がえられていない．今後は，筋力低下の関係する遺伝子の同定やCTGに対するアンチセンス療法[8]など，新しい治療法が期待されている．

※本論文に関連し，開示すべきCOI状態にある企業，組織，団体はいずれも有りません．

文　献

1) Udd B, Krahe R. The myotonic dystrophy: molecular, clinical, and therapeutic challenges. Lancet Neurology 2012;11:891-905.
2) Cho DH, Tapscott SJ. Myotonic dystrophy. Biochim Biophys Acta 2007;1772:195-204.
3) Mankodi A, Logigian E, Callahan L, et al. Myotonic dystrophy in transgenic mice expressing an expanded CUG repeat. Science 2000;289:1769-1772.
4) Koebis M, Kiyatake T, Yamaura H, et al. Ultrasound-enhanced delivery of morpholino with bubble liposomes ameliorates the myotonia of myotonic dystrophy model mice. Sci Rep 2013;3:2242.
5) Oana K, Oma Y, Suo S, et al. Manumycin A corrects aberrant splicing of Clcn1 in myotonic dystrophy type 1 (DM1) mice. Sci Rep 2013;3:2142.
6) Kino Y, Washizu C, Oma Y, et al. MBNL and CELF proteins regulate alternative splicing of the skeletal muscle chloride channel CLCN1. Nuc Acids Res 2009;37:6477-6490.
7) Wheeler T, Lueck JD, Swanson MS, et al. Correction of ClC-1 splicing eliminates chloride channelopathy and myotonia in mouse models of myotonic dystrophy. J Clin Invest 2007;117:3952-3957.
8) Wheeler T, Sobczak K, Lueck JD, et al. Reversal of RNA dominance by displacement of protein sequestered on triplet repeat RNA. Science 2009;325:336-339

Abstract

Myotonic dystrophy

Shoichi Ishiura, Ph.D.[1], Kosuke Oana, M.S.[1] and Michinori Koebis, M.S.[1]

[1]Graduate School of Arts and Sciences, The University of Tokyo

No effective treatment was available for myotonic dystrophy, even in animal model. We have established a new antisense oligonucleotide delivery to skeletal muscle of mice with bubble liposomes, and led to increased expression of chloride channel (CLCN1) protein and the amelioration of myotonia. In other experiments, we also identified small molecule compounds that correct aberrant splicing of *Clcn1* gene. Manumycin A corrected aberrant splicing of Clcn1 in mouse model.

(Clin Neurol 2013;53:1109-1111)

Key words: myotonic dystrophy, splicing, chloride channel, myotonia, therapy

Available online at www.sciencedirect.com

SciVerse ScienceDirect

Neuromuscular Disorders 23 (2013) 917–921

www.elsevier.com/locate/nmd

Case report

Fatal hepatic hemorrhage by peliosis hepatis in X-linked myotubular myopathy: A case report

T. Motoki [a,*], M. Fukuda [d], T. Nakano [a], S. Matsukage [b], A. Fukui [c], S. Akiyoshi [e], Y.K. Hayashi [f,g], E. Ishii [d], I. Nishino [f,g]

[a] *Department of Pediatrics, Uwajima City Hospital, Uwajima, Ehime, Japan*
[b] *Pathology, Uwajima City Hospital, Uwajima, Ehime, Japan*
[c] *Radiology, Uwajima City Hospital, Uwajima, Ehime, Japan*
[d] *Department of Pediatrics, Ehime University Graduate School of Medicine, Toon, Ehime, Japan*
[e] *Department of Neonatology, Ehime Prefectural Central Hospital, Matsuyama, Ehime, Japan*
[f] *Department of Neuromuscular Research, National Institute of Neuroscience, National Center of Neurology and Psychiatry (NCNP), Tokyo, Japan*
[g] *Department of Clinical Development, Translational Medical Center, NCNP, Kodaira, Tokyo, Japan*

Received 31 October 2012; received in revised form 4 May 2013; accepted 11 June 2013

Abstract

We report a 5-year-old boy with X-linked myotubular myopathy complicated by peliosis hepatis. At birth, he was affected with marked generalized muscle hypotonia and weakness, which required permanent ventilatory support, and was bedridden for life. He died of acute fatal hepatic hemorrhage after using a mechanical in-exsufflator. Peliosis hepatis, defined as multiple, variable-sized, cystic blood-filled spaces through the liver parenchyma, was confirmed by autopsy. To avoid fatal hepatic hemorrhage by peliosis hepatis, routine hepatic function tests and abdominal imaging tests should be performed for patients with X-linked myotubular myopathy, especially at the time of using artificial respiration.

Keywords: X-linked myotubular myopathy; Hepatic hemorrhage; Peliosis hepatis; Mechanical in-exsufflator

1. Introduction

X-linked myotubular myopathy (XLMTM) is one of the most serious types of centronuclear ("myotubular") myopathies, which is pathologically characterized by a high proportion of small myofibers with centrally placed nuclei [1]. With recent advances in molecular analysis, centronuclear myopathy has been classified into three genetic subtypes. XLMTM is a severe form of centronuclear myopathy presenting with symptoms from birth, including respiratory failure, ophthalmoplegia, and muscle weakness [2]. XLMTM is caused by genetic aberration of the *MTM1* gene on chromosome Xq28 [3]. *MTM1* encodes myotubularin, a dual-specificity 3-phosphoinositide phosphatase, which plays an important role in the regulation of signaling pathways involved in muscle growth and differentiation [3].

Although XLMTM is considered to be a fatal disorder within the first year of life, it has been recently shown that more than half of XLMTM patients achieve prolonged survival, and most of the long-term survivors suffer from several complications in several organ systems [4]. Among them, peliosis hepatis is a rare condition that can affect children and cause fatal hepatic hemorrhage. A few reports have suggested that XLMTM patients might be at risk for development of peliosis hepatis [4–7]. We report a 5-year-old patient with XLMTM who suffered

* Corresponding author. Address: Department of Pediatrics, Uwajima City Hospital, 1-1 Goten-cho, Uwajima, Ehime 798-8510, Japan. Tel.: +81 895 25 1111; fax: +81 895 25 5334.
E-mail address: tmotoki@m.ehime-u.ac.jp (T. Motoki).

0960-8966/$ - see front matter © 2013 Elsevier B.V. All rights reserved.
http://dx.doi.org/10.1016/j.nmd.2013.06.008

from fatal peliosis hepatis. In addition, the clinical features and prevention approach of fatal hepatic hemorrhage in XLMTM are also discussed.

2. Case report

A full-term male was born at 39 weeks of gestational age by normal spontaneous vaginal delivery and weighed 2728 g. The Apgar score was 5 at 1 min and 7 at 5 min. There was no abnormal antenatal symptom (e.g. polyhydramnios, reduced fetal movements, and thinning of the ribs). And neither family history of genetic disorders nor medical problem during perinatal period was observed. At birth, however, marked generalized muscle hypotonia and weakness, which required ventilatory support, appeared in the patient. On physical examination, facial muscle weakness and a high-arched palate were detected, and extraocular muscle involvement was not detected. The hypotonia did not improve with conventional management. The karyotype of peripheral blood was normal. A muscle biopsy from the biceps branch was performed under the possible diagnosis of neuromuscular disease. All muscle fibers were small and round (Fig. 1a), and a peripheral halo was observed in most fibers (Fig. 1b), compatible with the diagnosis of myotubular myopathy. Type 1 fiber predominance was remarkable (90%) (Fig. 1c). Genetic analysis of XLMTM revealed a splice-acceptor-site mutation of *MTM1* in intron 6 (c.445-1G>A), resulting in skipping of exon 7 at the cDNA level (Fig. 1d) [8]. The patient received respiratory support using non-invasive positive pressure ventilation, and underwent a tracheotomy at 8 months of age because of frequent asphyxia caused by aspiration.

At 5 years old, he was admitted to the Uwajima City Hospital for treatment of massive pneumonia and atelectasis in the left lung. Laboratory studies on admission showed that hemoglobin was 14.6 g/dL, white blood cell count was 11,400/μL, platelet count was 338,000/μL, aspartate aminotransferase was 69 IU/L, alkaline phosphatase was 73 IU/L, and C-reactive protein was 0.46 mg/dL. Bacterial blood and sputum cultures showed negative results. Fibrinolytic activity test on four days after admission remained within normal limits (prothorombin time was 11.9 s, fibrin degradation products was 8.6 μg/ml and D-dimer was 0.8 μg/ml). The patient gradually improved with a course of antibiotics (cefotaxime sodium) and lung physical therapy. Nine days after admission, a mechanically assisted coughing system was used as a mechanical in-exsufflator (MI-E) because of difficulty of sputum expectoration. The next day, he suffered from abrupt tachycardia and cyanosis. He had a peripheral coldness and his abdomen was gradually distended, especially the right costal margin, because of hepatic enlargement. Laboratory studies

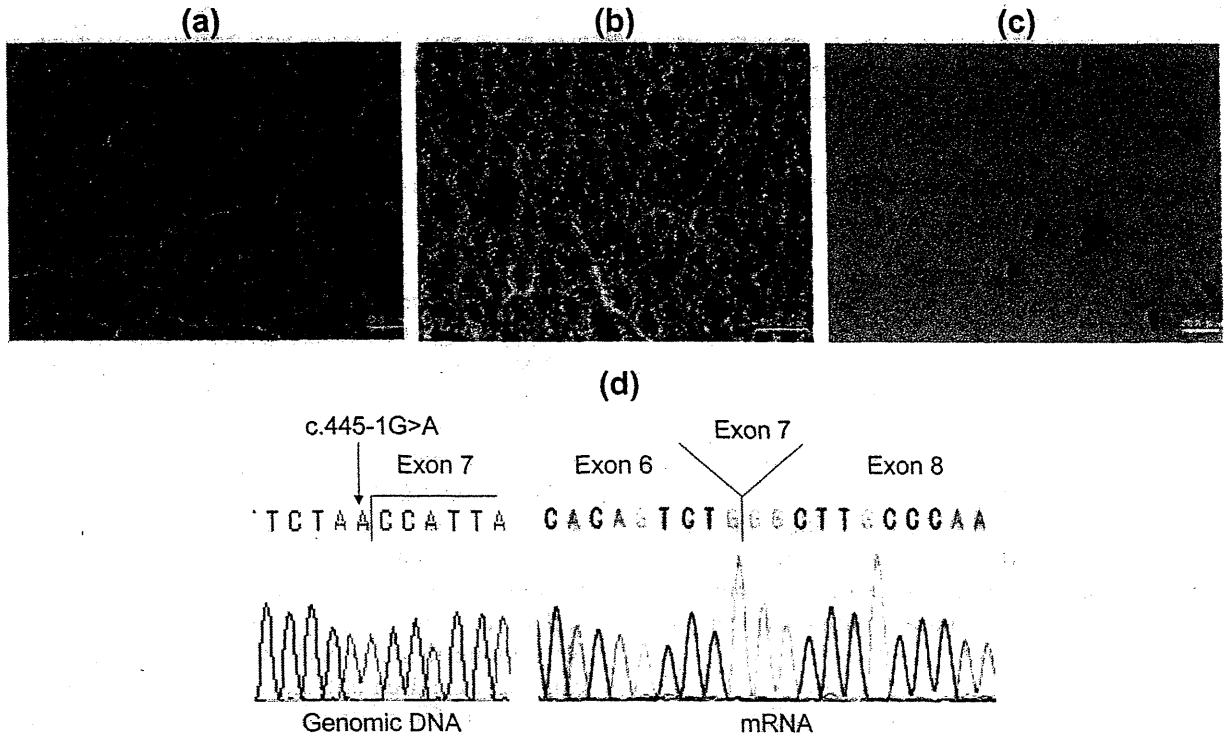

Fig. 1. Histological findings of muscle biopsy and genetic analysis. (a) Hematoxylin and eosin (H & E) staining shows that all muscle fibers are small and round. Marked perimysial fibrosis and scattered pyknotic nuclear clumps can be seen. Muscle fibers with central nuclei comprise 40% of the biopsy specimen. (b) As shown by nicotinamide adenine dinucleotide tetrazolium reductase staining, the intermyofibrillar network is markedly disorganized with peripheral halo features seen in most fibers. (c) On ATPase, types 1, 2A–C comprise 90%, 8%, 2%, and 0%, respectively. Type 2 fiber atrophy can be seen. (d) *MTM1* analysis revealed a splice-acceptor-site mutation in intron 6 (c.445-1G>A) at the genomic DNA level and skipping of exon 7 at the cDNA level.

showed that the hemoglobin level and platelet count were decreased to 6.4 g/dL and 82,000/μL, respectively. An abdominal computed tomography (CT) scan showed hepatomegaly with a heterogeneous low density area expanding from the medial segment to the right lobe of the liver, and the leakage of contrast material into parenchyma during the arterial phase, suggesting the diagnosis of liver hemorrhage (Fig. 2a). There was little intraperitoneal bleeding. With rapid transfusion of red cells, a hepatic angiogram was performed via the common hepatic artery. Because active bleeding was observed within liver parenchyma (Fig. 2b), obstructing material (Gelpart® Molecular Devices, Nippon Kayaku Co. Ltd., Tokyo, Japan) was injected into the anterior and posterior branches of the hepatic artery to control active bleeding. Despite these treatments, hemoglobin levels gradually decreased from 11.1 to 3.8 g/dL 8 h after the obstruction therapy. The abdomen was further distended and pitting edema appeared in the lower body. Repeated abdominal CT showed massive intraperitoneal bleeding compared with that of the previous day, and a narrowed inferior vena cava caused by hepatic enlargement was detected. He died 4 days after the onset of acute hepatic hemorrhage. The autopsy indicated

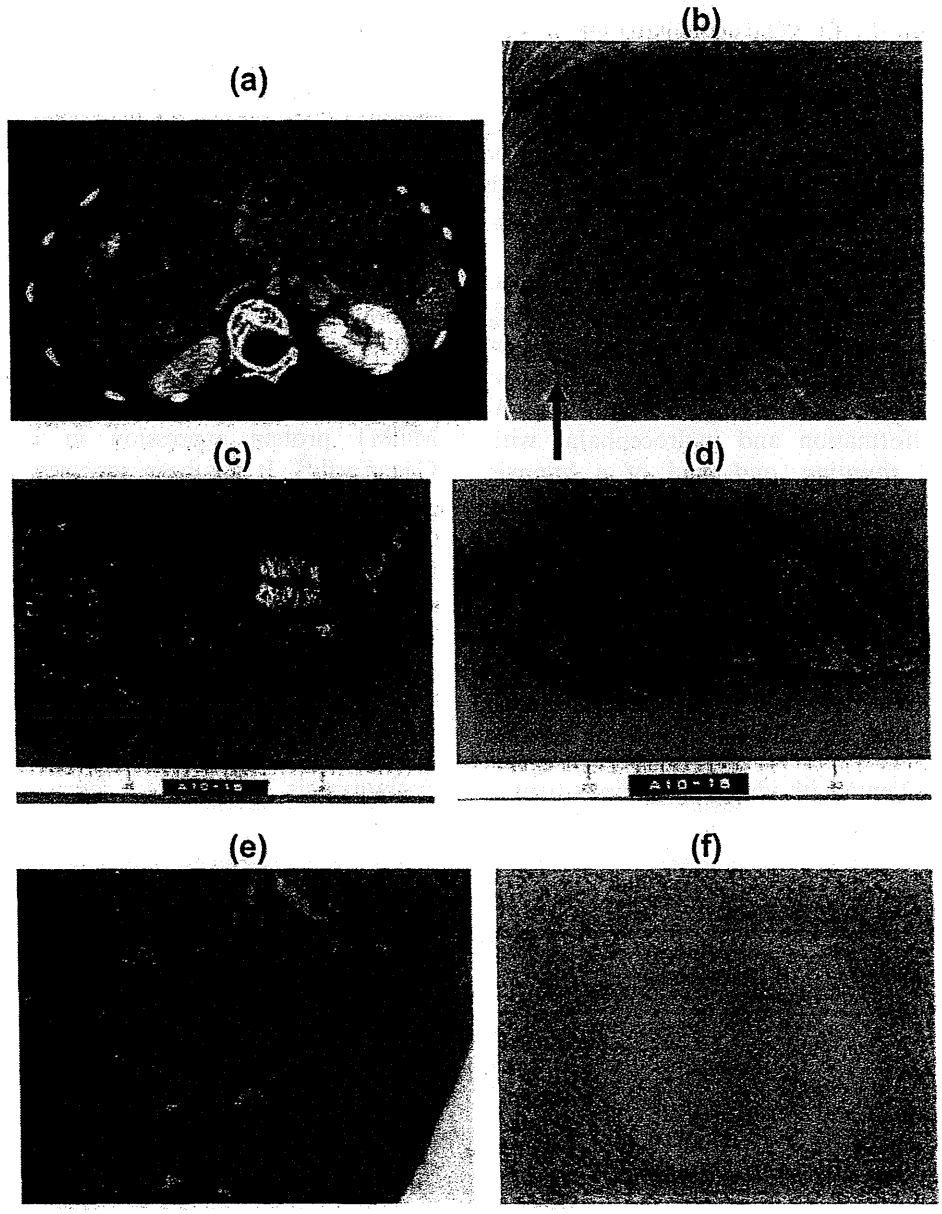

Fig. 2. Radiological and pathological findings of periosis hepatis. (a) Contrast abdominal CT shows hepatomegaly and a heterogeneous low density area extending from the medial segment to the right lobe of the liver. Contrast dye had leaked into the parenchyma (arrow) during the arterial phase. (b) A hepatic angiogram shows a number of retained contrast agents and some active bleeding (arrow) within liver parenchyma. (c and d) Autopsy findings show expansive intraperitoneal bleeding caused by rupture at the right hepatic capsule, and multiple variable-sized cystic blood-filled spaces were found in a section of the liver. (e) Multiple blood-filled spaces within the liver parenchyma can be seen (H & E). (f) Immunohistochemically, the inner surface of the blood-filled space is devoid of CD31-positive endothelial lining in contrast to the sinusoidal endothelia.

expansive intraperitoneal bleeding caused by rupture of the right hepatic capsule (Fig. 2c). Multiple variable-sized cystic blood-filled spaces and hemorrhagic necrosis were found in the liver (Fig. 2d). Histopathologically, the liver contained multiple blood-filled spaces (Fig. 2e) that were devoid of CD31-positive endothelial lining (Fig. 2f), which was compatible with peliosis hepatis.

3. Discussion

Peliosis hepatis is a rare fatal disorder with a number of causes, and is defined as multiple, variable-sized, cystic, blood-filled spaces through the liver parenchyma, in which spaces are not covered by endothelium of blood vessels histopathologically [9]. Peliosis hepatis has mostly been reported in adult patients associated with chronic wasting disorder [10], human immunodeficiency virus infection [11–12], oral contraceptives [13], androgenic steroids [14], and *Bartonella henselae* infection [15], and is idiopathic [16]. In children, peliosis hepatis is rare and has only been reported with androgenic steroids [17–18], *Escherichia coli* pyelonephritis [19], and XLMTM [4–7].

In XLMTM, only six children with peliosis hepatis, including our case, have been reported (Table 1) [4–7], and five of them developed acute onset multiple organ failure. The remaining child was detected by chance at the time of the autopsy, and this child had a central nervous system malformation and hydrocephalus with ventriculo-peritoneal shunting, and died of a hypoxic episode at 4 years old. The mean age at onset of peliosis hepatis was 4 years. Antecedent infection before hepatic hemorrhage was observed in three patients, including our patient. An elevated liver function test was observed in three patients, including our patient, but was normal in two. Five of six patients died of acute fatal hepatic hemorrhage. One patient survived after laparotomy and transarterial embolization [5]. Therefore, peliosis hepatis with XLMTM is characterized by difficult-to-treat acute onset. Some adult patients with idiopathic peliosis hepatis have received successful emergent hepatectomy, liver transplantation, and arterial embolization [16,20]. However, once hepatic hemorrhage from peliosis hepatis occurs, it is usually difficult to control bleeding, as observed in our patient. Therefore, reducing the incidence and prompt recognition of hepatic hemorrhage are mandatory for XLMTM patients.

The diagnosis of peliosis hepatis is difficult and often missed or delayed because of the atypical findings on standard radiological tests. A previous report indicated that ultrasonic examination is useful to detect abnormal findings according to various liver conditions, and can show perinodular and intranodular vascularity in patients with peliosis hepatis [21]. Other imaging systems, including CT, magnetic resonance imaging, and angiography can also be helpful for diagnosis of peliosis hepatis [18,21]. Our patient showed persistent mild elevations in a serum liver function test before the episode of acute hemorrhage. He had not received a routine ultrasonic examination, and CT findings on admission indicated no hepatic lesion, suggesting hemorrhage or peliosis hepatis. Therefore, fatal hepatic hemorrhage from peliosis hepatis was induced by an unknown cause after admission.

The mechanism of peliosis hepatis remains to be fully elucidated. And the causal relationship between peliosis hepatis and XLMTM is poorly understood, although MTM1 protein expression in liver are reported in GeneCards®. It has been reported that a mechanical in-exsufflator (MI-E) is safe and effective for respiratory infections of pediatric patients with neuromuscular disorders [22]. MI-E was initially used for removing secretions in our case, and fatal hepatic hemorrhage occurred on the next day of MI-E adoption. In some reports describing the mechanism of peliosis hepatis, blockade of liver blood outflow and increased sinusoidal pressure in patients with abnormality of the sinusoidal barrier were important factors contributing to the pathogenesis [23,24]. In our case, there were no

Table 1
Summary of peliosis hepatis in XLMTM patients.

No.	Age	Severity of XLMTM	Cognitive development	Detection of PH	Known liver dysfunction	Infection at the onset of PH	Diagnosis	Status
1[4]	5 y	Severe	Normal	Hepatic hemorrhage	Yes	Un-documented	Autospy	Deceased
2[4]	4 y	Severe	Normal	By chance (autospy)	No	Un-documented	Autospy	Deceased
3[5]	3 y	Severe/ moderate	Normal	Hepatic hemorrhage	No	URI otitis media	CT	Improved
4[6]	2 y 6 m	Severe	Un-documented	Hepatic hemorrhage	(Un-documented)	Un-documented	Autospy	Deceased
5[7]	5 y	Severe	Un-documented	Hepatic hemorrhage	Yes	Fever	Autospy	Deceased
6 (present patient)	5 y	Severe	Slightly retarded	Hepatic hemorrhage	Yes	Pneumonia	Autospy	Deceased

PH: peliosis hepatis, URI: upper respiratory infection, CT: computed tomography.